9-23-2010

ASSESSING PLASTICITY: THE POPULATIONS RESPONSIBLE FOR THE EPITHELIAL ENGRAFTMENT OF MARROW-DERIVED CELLS

Justin Brent Cohen
Yale University

ASSESSING PLASTICITY: THE POPULATIONS RESPONSIBLE FOR THE EPITHELIAL ENGRAFTMENT OF MARROW-DERIVED CELLS

A THESIS SUBMITTED TO THE YALE UNIVERSITY SCHOOL OF MEDICINE IN PARTIAL FULFILLMENT OF THE REQUIREMENTS FOR THE DEGREES OF DOCTOR OF MEDICINE AND MASTER OF HEALTH SCIENCE

BY

JUSTIN BRENT COHEN

2010

ABSTRACT

Bone marrow-derived cells (BMDCs) have significant plasticity allowing them to give rise to various non-hematopoietic cell types including epithelial cells of the lung, liver, gut, and skin. These findings offer tremendous possibilities for the use of cell therapy to treat tissue injury and disease. However, the specific populations of cells responsible for this phenomenon are still unclear with considerable controversy over the mechanism of this transformation.

In this study, we sought to compare the epithelial engraftment ability of two populations enriched for hematopoietic stem cells (HSCs), specifically the fractionated, lineage-depleted, and homed subset (FLH) and the lineage^{-}Sca-1^{+}c-Kit^{+} sorted population (LSK), to whole bone marrow (WBM). Plasticity capability was assessed by examining the engraftment of type II (T2) pneumocytes in the lung following sex-mismatched bone marrow transplantation in mice. The recipient mice were knockouts of surfactant protein C (SPC), a T2-specific protein, thereby allowing detection of the transplanted wild-type cells in the lung using immunofluorescence for SPC on paraffin sections and cytospins. Additionally, quantitative PCR (qPCR) for SPC transcripts provided a sensitive method of detecting engraftment of these BMDCs.

Our data suggest that the FLH and LSK populations engraft in the lung at least as well as the control WBM. Despite our effective detection techniques, only exceedingly rare donor-derived T2 cells could be found by both microscopy and qPCR. Therefore, fluorescence-activated cell sorting (FACS) of the digested lung was tested and found to be reliable in isolating and enriching for these conversion events.

Vav ancestry mice were also utilized in a similar transplantation model to directly evaluate the engraftment ability of the hematopoietic and non-hematopoietic fractions of the bone marrow. Preliminarily, the hematopoietic populations showed higher levels of epithelial engraftment by both immunofluorescence and qPCR. Interestingly, a second dose of targeted lung irradiation was necessary to elicit this effect suggesting that greater levels of tissue damage may be necessary for this model's success.

When taken as a whole, our results seem to implicate HSC subpopulations as enriched for highly plastic cells which are able to engraft as T2 cells in the lung. The mechanism behind this conversion still remains to be studied but we hypothesize that both cell fusion and incidental entrapment of transplanted BMDCs are responsible.

ACKNOWLEDGEMENTS

First off, I would like to thank my adviser Diane Krause. You have completely embodied the role of a mentor. I am greatly appreciative for the time, effort, and attention you gave to both my project and my career. In so doing, you have showed an incredible commitment to teaching and my education. I have learned innumerable lessons during my past years in the lab, and I hope that we will continue to be colleagues and friends in the coming years.

I would also like to express my gratitude to Susannah Kassmer for being willing to discuss every aspect of this project. You always provided ample help and insightful suggestions during this journey. I wish you the best in your own career.

My time in the lab would not have been so productive if it wasn't for the congeniality and assistance of the other members of the Krause lab: Sharon, Manu, Kate, Lin, Ping-xia, Yuan, Crew, Stephanie H, Stephanie M, Stephanie D, Sofya, and Pat.

I am grateful to my thesis committee of Erica Herzog, Bernie Forget, and Peter Tattersall for their feedback and readiness to improve this work.

Most importantly, I would like to thank my parents for their unwavering love and support. Without you, I never would have been able to achieve this milestone. I simply cannot repay you for the devotion and caring that are so obvious in everything you do to make my life easier.

Finally, I would like to acknowledge the generous financial support from The Howard Hughes Medical Institute Medical Fellows Program in addition to the National Institutes of Health-NHLBI Medical Student Research Fellowship. Thank you also to Donna, Mae, and Dr Forrest in the Office of Student Research for the facilitating the completion of this project.

TABLE OF CONTENTS

INTRODUCTION

Lung Structure and Function

The lung's primary function is to exchange gases, predominantly oxygen and carbon dioxide, between inspired air and blood. This respiratory function occurs in the distal most regions of the lung in alveolar sacs that are the blind ends of the lung parenchyma but contiguous with the outside world. Alveoli are the site of gas exchange and, in cross-section, appear open and with incomplete walls. There is a rich capillary network associated with each alveolar sac. To separate the capillary endothelial cells from the alveolar lining epithelial cells, there exists a very thin basement membrane and surrounding interstitial tissue.

Alveolar epithelium itself is a continuous layer composed of two principal cells types: type I and type II pneumocytes. Type I cells appear flattened, plate-like, with small nuclei, scant cytoplasm and cover 95% of the alveolar surface while comprising only 8% of the total cells in the lung. This specialized morphology makes these cells highly optimized for gas exchange. In contrast, type II (T2) cells are secretory cells with osmiophilic lamellar bodies containing surfactant. In addition to producing surfactant, T2 cells are the main cell type involved in the repair of alveolar epithelium after destruction of type I cells. It is for this reason that T2 cells are sometimes considered the intra-organ stem cells of the respiratory unit since they can give rise to type I cells along with additional type II cells.

Alveolar macrophages also reside in the alveoli loosely attached to the epithelial cells or lying free within the alveolar spaces. Microscopically, these macrophages are large, pleomorphic, and heterogeneous in cell shape and surface morphology. These cells are derived from blood monocytes and belong to the mononuclear phagocyte system. They are often filled with carbon particles and other phagocytosed material (1).

Surfactant Protein C (SPC)

Pulmonary surfactant is a complex mixture of lipids and proteins that reduces surface tension, increases compliance, minimizes fluid accumulation, and maintains alveolar size (2). Surfactant is secreted at the air-fluid interface in the lung by T2 pneumocytes along with the non-ciliated columnar epithelium of the larger airways. The surfactant apoprotein itself is bound to the lipid dipalmitoylphosphatidylcholine such that secreted surfactant contains both hydrophobic and hydrophilic regions. While surfactant proteins A, B, and D have been detected in multiple organs (such as the blood and gastrointestinal tract), surfactant protein C mRNA and protein have only been noted to be produced and secreted by the T2 cell in the lung (3). This makes SPC an ideal reporter protein for type II pneumocyte structure and function.

Whereas surfactant protein B (SPB) gene deletion is lethal in early life (4), SPC knockout mice demonstrate a more subtle phenotype in which there are abnormalities in lung elasticity and stabilization of other surfactant proteins. In

humans, SPC deficiency results in adult onset interstitial lung disease that may be related to abnormal processing of SPC protein which leads to its accumulation in T2 cells (5). The murine models mirror this result with chronic inflammation leading to increased lung fibrosis, emphysema, and dysplastic T2 cells (6, 7).

Stem Cells

Stem cells hold great promise for the future approaches to medicine in the areas of regenerative medicine, cell-based tissue repair in cancer treatment, and gene therapy (8). Many tissues are candidates for therapeutic treatment but a better understanding of general biological principles in these unique cells is necessary before this vision can materialize (9). Even with our currently incomplete level of understanding, the biology of hematopoietic stem cells in particular has led to a number of medical advances in cancer therapy, transplantation, and autoimmunity.

Stem cells are biological units which are responsible for the development and regeneration of tissues and organ systems. Since the 1960s, stem cells are generally defined as clonogenic cells, which are capable of both self-renewal and multilineage differentiation at the single cell level (10). There are many categories of stem cells, which are mostly human semantic constructions to deal with the complexity of these diverse entities. Stem cells can be divided into a long-term subset, capable of infinite self-renewal, as well as a short-term subset that self-renews for a defined interval. Stem cells also undergo differentiation and must give rise to non-self renewing oligopotent progenitors. The earliest stem cells in ontogeny (those from

the zygote to the inner cell mass of the blastocyst) are classified by their developmental potential as totipotent meaning that they are able to give rise to all embryonic and extra-embryonic cell types. Embryonic stem cell lines, which are derived from the inner cell mass of the gastrula, are considered pluripotent in that they can give rise to all three germ layers of the embryo but not the extra-embryonic tissues. Adult stem cells are believed to be more restricted in their differentiation ability and merely able to regenerate specific cells types within a tissue; type II pneumocytes of the lung, gastrointestinal crypt cells, and oval cells of the liver demonstrate this capacity.

Hematopoietic Stem Cells

Hematopoietic stem cells (HSCs) are a well-studied population, with a single HSC being capable of reconstituting the entire hematopoietic system following an otherwise lethal dose of radiation (11). These HSCs are very rare in mice and account for approximately 1 in 100,000 nucleated cells in the bone marrow (12-14). In order to study and characterize these cells, multiple isolation protocols have been developed. Typically these protocols begin with a lineage deletion step in which cells displaying surface markers consistent with mature lineages are removed. The lineage removal antibody cocktail contains Ter-119 for erythrocytes, CD11b for macrophages and granulocytes, CD3 for T-cells, and B220 for B-cells. This resulting lineage-negative population is enriched for HSCs 10- to 100-fold. This lin- population can then be further purified for HSCs using CD34+ cells (15), c-

$Kit^{+}Thy1^{lo}Sca\text{-}1^{+}$(KTLS) (16), or exclusion of rhodamine and Hoechst dyes ($Rhodamine^{lo}Hoechst^{lo}$) (17). But cell surface markers are not the only way to isolate potential HSCs. A protocol which utilizes cell migration and survival involves purifying lin- cells, and then separating this population based on size using an elutriator. These cells are then injected into a lethally irradiated recipient mouse. After 48 hours the cells that were able to home to the bone marrow are collected as so called elutriated, lineage-depleted, and homed cells (ELH) (18). A single KTLS or ELH cell can provide long-term hematopoietic reconstitution in about 20% of lethally irradiated mice (16, 19).

The same purification techniques that enrich for HSCs also enrich for cells that are capable of engraftment as epithelial cells. Since there is no evidence yet that these cells were ever committed to hematopoiesis prior to their differentiation into epithelial cells, these cells will be referred to as bone marrow-derived cells (BMDC), and cells that are committed to hematopoiesis (e.g. KTLS) as HSCs. Until it is proven that a cell can be committed to hematopoiesis, and then differentiate into a mature functional epithelial cell without fusion, the term “transdifferentiation” will not be used.

Plasticity

Many exciting discoveries have demonstrated that BMDCs have more potential than previously suggested. In fact, they have been shown to develop into tissue specific cells in the lung (19-23), heart (24), brain (25), skeletal muscle (26,

27), bone (28), liver (29, 30), kidney (31, 32), pancreas (33, 34), eye (35), skin (36), and gastrointestinal tract (37). This phenotypic flexibility is termed "plasticity" and refers to the ability of adult stem cells to cross lineage barriers and adopt the expression profiles and functional characteristics of cells unique to other tissues. In 1999, this transformation phenomena was first noticed in lethally irradiated female rats and mice that had received male bone marrow cells. When examining the livers of these animals, Y chromosome-positive hepatocytic oval cells were noted (30, 38). This data has since been corroborated but with widely varying engraftment rates of 0.01 to 2%. This discrepancy is most likely due to the differences in experimental conditions such as the number and type of cells transplanted, the methods of detection, and the degree and type of liver injury. As more sophisticated methods of detection were developed to reduce cell overlay and exclude blood and endothelial cells (with CD45 and cytokeratin staining), the donor-derived hepatocyte engraftment rate was revised to approximately 0.1% (39).

The Importance of Tissue Damage in the Lung

Many of these previous studies utilize some form of organ injury to induce engraftment in mice. The best studied mechanism for lung damage is ionizing total body irradiation at lethal levels greater than 1,000 cGy. At this dose, severe lung injury occurs as demonstrated by capillary breakdown and extravasation of erythrocytes into the alveolar spaces. This damage worsens from day 0 to day 5 with restoration of alveolar septal integrity by about day 7. This high level of injury

is necessary for BMDC to engraft as lung epithelial cells while lower doses of greater than 400 cGy were conducive to high rates of hematopoietic engraftment (40). This data demonstrate a threshold effect for inducing lung damage such that BMDC can engraft in this niche.

Bleomycin is another agent which has been used to induce lung injury. Bleomycin is a glycopeptide antibiotic, which is used clinically as a chemotherapeutic. However, it is also one of the most extensively studied and reproducible experimental models for lung fibrosis. When bleomycin is delivered into the airway, it produces acute lung epithelial injury, followed by a prolonged inflammatory response which leads to lung fibrosis that eventually resolves (41).

Bone Marrow-Derived Cells in the Lung

Early work in the field of lung engraftment demonstrated that bone marrow cells (specifically mesenchymal precursor cells) could adopt a collagen producing phenotype in the murine lung (42). However, the first evidence that BMDCs could become lung epithelial tissue was published in 2001 (19). These experiments used lethally irradiated mice which were then transplanted with a single sex-mismatched ELH HSC. At the time of sacrifice 11 months later, multiple epithelial compartments were populated with Y chromosome containing cells which must be the progeny of this originally transplanted ELH cell. In particular, the bronchi and alveoli showed a significant amount of engraftment (12.58% and 2.32%, respectively). This outcome was observed using colocalization of FISH staining for Y chromosome along with

either FISH for SPB or immunostaining for SPB. However, a follow-up study by a different group utilizing multiple different methods (e.g., starting donor cell, detection methods, timing at sacrifice) was unable to reproduce these results (43).

Mirroring the initial findings by Krause et al (19), Theise et al (22) used the CD34+Lin- subset of HSCs and a shorter time to sacrifice of 5 days to 6 months. They found similar results that donor-derived cells had engrafted as 2%-14% of the total type II pneumocytes. Grove et al (21) expanded the clinical implications of these techniques by demonstrating that HSCs could be delivery vehicles for gene therapy. They used whole bone marrow enriched for HSCs using 5-FU and then retrovirally transfected the eGFP gene before systemically injecting the cells into a irradiated host. Donor-derived T2 cells, which also stably expressed eGFP, were found in all recipients at time points from 2 to 11 months.

In contrast to these results, Kotton et al (20) intravenously delivered lacZ-labeled, plastic adherent mesenchymal stem cells (MSCs) after bleomycin-induced lung injury. They detected marrow-derived cells engrafted as type I cells by morphological and molecular phenotype but no T2 pneumocytes. Using the same model, Ortiz et al (23) showed that donor MSCs localized to the zones of bleomycin tissue injury and reduced fibrotic and inflammatory damage. However, the low numbers of donor-derived cells engrafting the lung did not appear sufficient to account for the therapeutic response, suggesting that donor stem cells may have other local effects mediated through paracrine factors (44).

Nevertheless, there are numerous studies to the contrary utilizing discernibly different methods to demonstrate a lack of plasticity for adult stem cells. Wagers et al (43) used two approaches to test their hypothesis: a chimeric mouse produced via bone marrow transplantation with GFP-expressing KTLS HSCs, and parabiotic animals which joined the circulation of a transgenic GFP mouse and a wild type mouse. Both groups had the expected reconstitution or chimerism in their hematopoietic system, but there was very little evidence for plasticity and engraftment. In the transplantation approach, only 1 cell in 13.2 X 10^6 in the brain and 7 cells out of 4.7 X 10^6 in the liver expressed the donor GFP marker. Furthermore, there was no evidence of epithelial engraftment in the lung. Similarly, the parabiotic model demonstrated no HSC engraftment beyond the hematopoietic system. But this result is not surprising given the need for tissue damage to elicit engraftment as explained above.

Kotton et al (45) used an SPC-eGFP reporter mice as a donor and transplanted either whole bone marrow or side population (SP) cells, which are also enriched for HSCs. So called SP cells have the unique ability to efflux Hoechst dye, and when examined by fluorescence-activated cell sorting (FACS) analysis they fall within a separate population that is to the "side" of the rest of the cells on a dotplot of emission data. Three months following irradiation, the mice were analyzed and, while they had good hematopoietic reconstitution, there was no evidence of donor cells being T2 pneumocytes by either FACS, fluorescence microscopy, or real-time PCR.

Chang et al (46) added to the field by discovering that these supposedly SPC and eGFP coexpressing cells were in fact microscopic artifact. Using deconvolution

microscopy, which is able to render a three dimensional image of the lung, these initially engrafted cells were actually false positives with endogenous SPC signal residing just outside of the donor-derived eGFP expressing cells with less than 300 nm separating the two.

An important aspect of plasticity studies is the number of variables which can affect the conversion outcomes; the timing of the transplant and analysis, the cell dose and number of cell infusions, the method of cell delivery, the functional state of the marrow cell delivered, and the nature of the marrow population or subpopulation are all influential. It should be noted that many of these negative studies utilized GFP transgene expression alone, which has been shown to be a relatively insensitive method of detection for BMDC lung epithelium because of inconsistent expression (47). Current standards in this field demand either confocal or single-cell analysis of marrow-derived epithelial cells to rule out the possibility of overlay. The addition of CD45 for hematopoietic antigens to staining protocols is appropriate along with phenotypic analysis of epithelial cell-specific markers to reduce microscopy artifact (39). A summary of publications on this topic can be seen in Table 1.

	Cells/route	Damage model	Findings	
MSC	IV	Irradiation	Engraftment of collagen transgene producing cells	(42)
	IV	Bleomycin	Type I (potential artifact)	(20)
	In vitro	Co-culture	BMDE, fusion	(48)
	IV	Bleomycin	Engraftment (epithelial-like cells)↑ w/ Bleo ↓ Fibrosis	(23)
	IV 6h post Bleo	Bleomycin ± busulfan	↑ Survival/repair ↑ G/GM-CSF ↓ Inflammatory cytokines	(49)
	In vitro	Co-culture	Epithelial-like morphology, CFTR+ epithelial cells in vitro	(50)
	IV (WBM too)	Naphthalene	Rare airway epithelial cells (CFTR+)	(51)
	IT	LPS IT	↑ Survival/repair ↓ Inflammation/edema	(31)
	IV	IP LPS	Prevention of LPS induced inflammation/injury/edema	(52)
Adh BM	Adherent BM (7d)	IP Naphthalene	BMDE cells identified after damage	(53)
WBM/HSC	IV	Irradiation	Rare BMDE cells	(54)
	IV	Irradiation	BMDE by concurrent Y-FISH, CK, and SPB	(19)
	IV	Irradiation	BMDE by concurrent Y-FISH, CK, and SPB	(22)
	IV	Irradiation	GFP+ alveolar epithelial cells	(21)
	IV	LPS	GFP+ alveolar epithelial cells	(55)
	IV	Irradiation	No BMDE	(43)
	Parabiosis	None		
	IV	Irradiation	No BMDE	(45)
	IV	Irradiation	No BMDE (deconvolution microscopy revealed false positive cells)	(46)
	SP/IV	Polidocanol IT	0.83% tracheal epithelium	(56)
	IV (rat) BMT	Asbestos	Epithelial cells, BADJ localization	(57)
	IV (human) BMT	Chemotherapy	Epithelial cells, endothelial cells	(58)
	IV (SP cells)	Irradiation	Type I, alveolar cells, rare bronchial epithelium, but not Type II engraftment	(59)
	IV	Radiation + elastase	↑ Engraftment and BMD cell repair following ATRA and G-CSF treatment	(60)
Other	Parabiosis	Radiation ± elastase	Type I cells	(61)
	Circulating precursor	Tracheal transplant	Recipient-derived epithelial cells	(62)
	Type II IT	Bleomycin	Decreased fibrosis, Y+ cells localized to fibrosis	(63)
	Circulating precursor	Lung transplant (human)	Epithelial cells	(64)
			Epithelium in bronchi and alveoli	(65)

Table 1: Summary of Publications Discussing Bone Marrow-Derived Epithelial Cells in the Lung

Figure adapted from Krause (66). References are in the last column. Abbreviations: intravenous (IV), intratracheal (IT), intraperitoneal (IP), bone marrow transplantation (BMT), Bleomycin (Bleo), Y chromosome positive (Y+), side population (SP), hematopoietic stem cell (HSC), whole bone marrow (WBM), bone marrow derived epithelial cell (BMDE), day (d), cytokeratin (CK), surfactant protein B (SPB), alveolar macrophage (AM), lipopolysaccharide (LPS), granulocyte colony stimulating factor and granulocyte macrophage colony stimulating factor (G/GM-CSF), broncho-alveolar duct junction (BADJ), all-trans retinoic acid (ATRA). All studies performed in mice except where indicated.

Bone Marrow-Derived Epithelial Cells in Humans

The appearance of bone marrow-derived epithelial cells is not just a research anomaly seen in experimental animals. When liver tissue from two women who had undergone bone marrow transplantation from male donors was examined, Y chromosome-positive hepatocytes could be identified in up to 12% of the liver specifically around the periportal area (67). Interestingly, the highest rates of engraftment could be seen in a separate patient who had developed recurrent hepatitis C infection. This again demonstrates that severe tissue injury can serve as a necessary impetus for significant engraftment.

With regards to the lung, Suratt et al studied (58) lung specimens from biopsy or autopsy from two female patients that had pervious sex-mismatched bone marrow transplants. They found chimerism in the alveoli with donor-derived epithelium (2.5-8.0%) and endothelium (37.5-42.3%) when merging images for Y chromosome FISH along with immunohistochemistry for cytokeratin (epithelial marker) and CD31 (endothelial marker). Of interest, there was a third patient examined in this series which did not demonstrate epithelial or endothelial chimerism but this patient was unique in that she had not received a conditioning regimen of total body irradiation. These findings have been echoed in other experiments in which lung transplantation recipients were seen to have recipient-derived type II (9.1-20%), bronchial epithelial (5.7-25.5%), and glandular (9.1-24.2%) cells (65). These robust results have since been tempered in a more recent study which demonstrated T2 cellular engraftment in the lung to be between 0% and 0.55% (68).

Functional Effects of Bone Marrow-Derived Cells

Although there has been significant discussion concerning the importance of these plasticity observations (69), in at least a few models it has been shown that these BMD epithelial cells can be quantitatively significant and functionally relevant. Lagasse et al (70) used a fumarylacetoacetate hydrolase (FAH) knockout mouse, which is an experimental model for hereditary tyrosinemia type 1. These mice necessarily die from liver failure due to the buildup of toxic metabolites of tyrosine. Amazingly, purified FAH+ KTLS HSCs and adult bone marrow cells could produce large numbers of functional hepatocytes (30-50% of liver mass) that were able to restore the biochemical function of the liver and rescue the mice from liver failure and certain death.

Orlic et al (24, 71, 72) have also shown that directly injected whole bone marrow or c-kit+ BM cells could restore some cardiac function in mice with myocardial infarctions. The Krause lab has published data proving that BM-derived gut epithelial cells can partially restore functional electrophysiological activity to the GI tract of cystic fibrosis transmembrane regulator (CFTR) knockout mice (73). Additionally, Zhao et al (74) demonstrated that human BMDCs can ameliorate stroke manifestation in rats. Interestingly, the beneficial effects of these cells in ischemia injury are not necessarily due to epithelial engraftment but rather could be the result of altered cytokine expression or engraftment as endothelial cells. This source of controversy remains an open question.

BMDCs have also been shown to be beneficial in a model of ischemic renal disease by differentiating into renal tubular cells (75). Wild-type mice underwent BM transplantation using $Lin^{-}Sca\text{-}1^{+}$ cells ubiquitously expressing β-galactosidase, and then were subjected to a period of renal ischemia by surgical clamping of the renal artery. The normal rise in blood-urea-nitrogen (BUN) concentrations induced by renal ischemia was significantly reduced in mice after transplantation with the $Lin^{-}Sca\text{-}1^{+}$ cells compared with controls. Furthermore, β-galactosidase-positive renal tubule epithelial cells were present as early as 48 hours after ischemic injury, which correlated with the protective effect. In contrast, no β-galactosidase-positive renal tubules were present in mice whose renal ischemia was preceded by the transplantation of Lin+ cells. The epithelial phenotype of the β-galactosidase-positive cells was confirmed by immunohistochemistry for megalin (a surface marker of tubular epithelia) and the lack of CD45 expression.

Functional effects of BMDCs in the lung have also been demonstrated. Inflammatory responses induced by either lipopolysaccharide (55) or elastase (60) could be reduced in the lung with the supplementation of BMDCs. Both of these papers used radiation conditioning as a precursor to bone marrow transplantation. It is suggested that the improvement in respiratory pathology is due to the temporary engraftment of type I, type II, and endothelial cells. However, both these studies have weaknesses because they lacked relevant non-irradiated controls.

A significant survival advantage was also conferred by administering BMD mesenchymal cells into mice that were myelosuppressed and then injured with

bleomycin (49). In these mice, BMDCs engrafted as both type I and type II pneumocytes. This protection was also associated with increased circulating levels of G-CSF and GM-CSF (known for their ability to promote the mobilization of endogenous stem cells) and with a decrease in inflammatory cytokines. However, this study raises the question whether epithelial engraftment itself or induction of reparative growth factors played the major role in protection from injury and fibrosis. All these studies seem to suggest that engrafting BMDCs are most beneficial in response to acute injury caused by genetic deficiency, infarction, or exogenous toxin. A summary of relevant literature is again presented in Table 1.

Vav Ancestry Mice

The vav protein was first described as an adapter protein based on its SH3 domains without an obvious enzymatic domain. However, it has since been determined that vav also plays critical roles in signaling via GTPase and other pathways (76). The particular usefulness of the vav protein promoter sequence lies in the demonstration that only cells committed to hematopoiesis express this sequence. Stadtfeld et al (77) first created transgenic mice, called vav ancestry mice, that express Cre recombinase on the vav promoter. When the vav ancestry mice are crossed with a Cre reporter strain that expresses YFP only after Cre-mediated excision, any cell that ever expressed vav would permanently express YFP (unless there was chromosomal deletion or promoter inactivation).The investigators used this tool in an effort to directly test whether cells that have committed to the

hematopoietic lineage are able to differentiate into epithelial cells normally in vivo. They hypothesized that if cells committed to hematopoiesis became hepatocytes or endothelial cells in vivo, then YFP-positive cells would be detectable over time without the need for tissue injury. Indeed they did find a very rare YFP+ hepatocyte (1/75,000) but no YFP+ endothelial cells.

STATEMENT OF PURPOSE

Bone marrow-derived cells have significant plasticity allowing them to give rise to various non-hematopoietic cell types including epithelial cells of the lung, liver, gut, and skin. These findings offer tremendous possibilities for the use of cell therapy to treat tissue injury and disease because BMDCs may represent a renewable pool of epithelial precursors. At present, bone marrow to epithelial cell engraftment levels in the lung are too low to be of clinical relevance. However, if these levels could be increased, there could be multiple therapeutic implications of this work. By better understanding the capabilities of subpopulations involved and the mechanisms by which they become epithelial cells, we will be able to design strategies to increase engraftment of these cells. Theoretically autologous BMDCs with the capacity to differentiate into mature pulmonary cells could be isolated and cultured in vitro to serve as target cells for gene therapy or as a resource for organ reconstitution and repair. However, selective long-term delivery of genes to the lung has not yet been highly successful. The immediate targets of these gene therapy projects could include inherited diseases of the respiratory tract such as surfactant protein deficiencies, cystic fibrosis, idiopathic pulmonary fibrosis, or α-1 antitrypsin deficiency.

Based on currently available evidence in the murine model, it is not clear if purified stem cell populations offer an engraftment advantage in the lung compared to whole bone marrow. Therefore, we designed an experiment to compare the use of

whole bone marrow to ELH and LSK populations to determine if any one group offers a higher conversion rate. A summary of experimental design is presented in Figure 1. Using SPCKO mice as recipients and WT mice as donors for transplantation, SPC mRNA and protein can be used as a donor-derived T2 pneumocyte cell marker measuring engraftment. Untransplanted SPCKO and WT mice were included as negative and positive controls, respectively. Additionally as a negative control for transplantation and radioprotection cell effects, SPCKO whole bone marrow cells were transplanted into an SPCKO recipient. The mice were sacrificed and analyzed three months later. We hypothesize that the ELH population by virtue of its homing ability will show improved engraftment when compared to WBM and LSK populations.

In this investigation, SPC production was detected by using immunofluorescence on paraffin and cytospin digestions of the lung. To complement these studies, quantitative PCR for SPC was utilized on the digested lung. These mice were also assessed for hematopoietic engraftment.

In an effort to investigate a better detection strategy for these rare BMD T2 cells, FACS analysis from GFP-positive donor mice into wild-type recipients was tested. The resulting donor-derived lung cells were then examined by confocal microscopy.

Lastly, to explore the potential of different BMD populations, the vav ancestry mice were used as donors into lethally irradiated SPCKO recipients. Specifically, this design allowed a comparison of engraftment capability between hematopoietic and

non-hematopoietic cell types, which are both resident in the bone marrow. The hematopoietic and non-hematopoietic fractions were divided based on vav-YFP expression using FACS. Again SPC mRNA and protein were used as a donor-derived T2 cell marker. The WBM population served as the control. The mice were sacrificed and analyzed one month later. We hypothesize that the YFP+ population representing the hematopoietic population will show better engraftment based on the previously purported plasticity of HSCs. Additionally, this transplantation model was used to determine if engraftment of these donor cell groups could be enhanced through a second dose of targeted lung irradiation. A summary of this experimental design is presented in Figure 2. We hypothesize that a second round of irradiation could further enhance engraftment by inducing additional damage and opportunities for BMDCs to engraft.

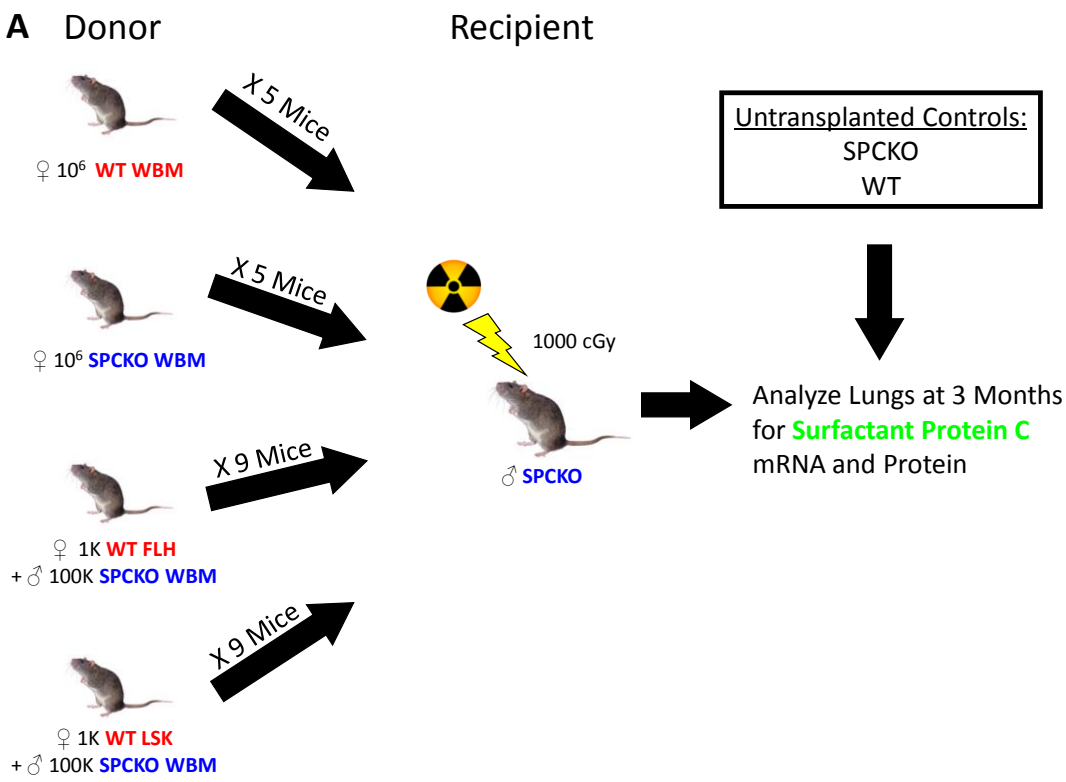
A
Donor
Recipient
X 5 Mice
♀ 10⁶ WT WBM
X 5 Mice
♀ 10⁶ SPCKO WBM
X 9 Mice
♀ 1K WT FLH
+ ♂ 100K SPCKO WBM
X 9 Mice
♀ 1K WT LSK
+ ♂ 100K SPCKO WBM
1000 cGy
♂ SPCKO
Untransplanted Controls:
SPCKO
WT
Analyze Lungs at 3 Months
for Surfactant Protein C
mRNA and Protein

B

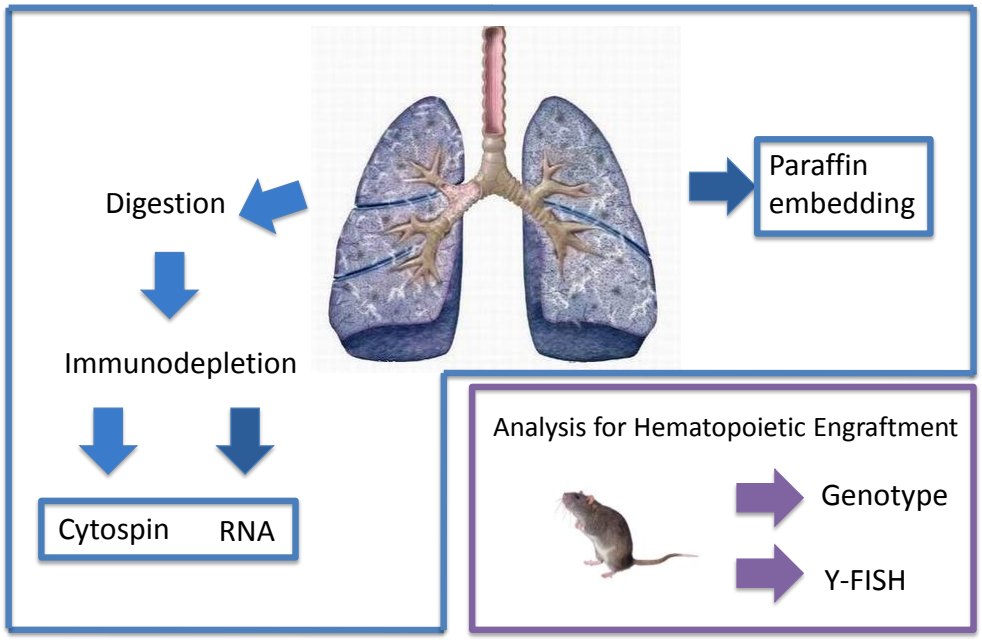

C

SPC	CD45	Interpretation
+	-	Engrafted Type II Pneumocyte
+	+	Contaminating Macrophage
-	+	Hematopoietic Cell
-	-	Other Cell Type

Figure 1: Schematic Showing the Experimental Design and Analysis

Panel A presents the transplantation scheme. NB The number of transplanted mice is not equal to the final number of mice analyzed due to expected animal loss.

Panel B shows the analysis steps for each animal.

Panel C is a table showing the interpretation of immunofluorescence patterns of lung cells seen under microscopy.

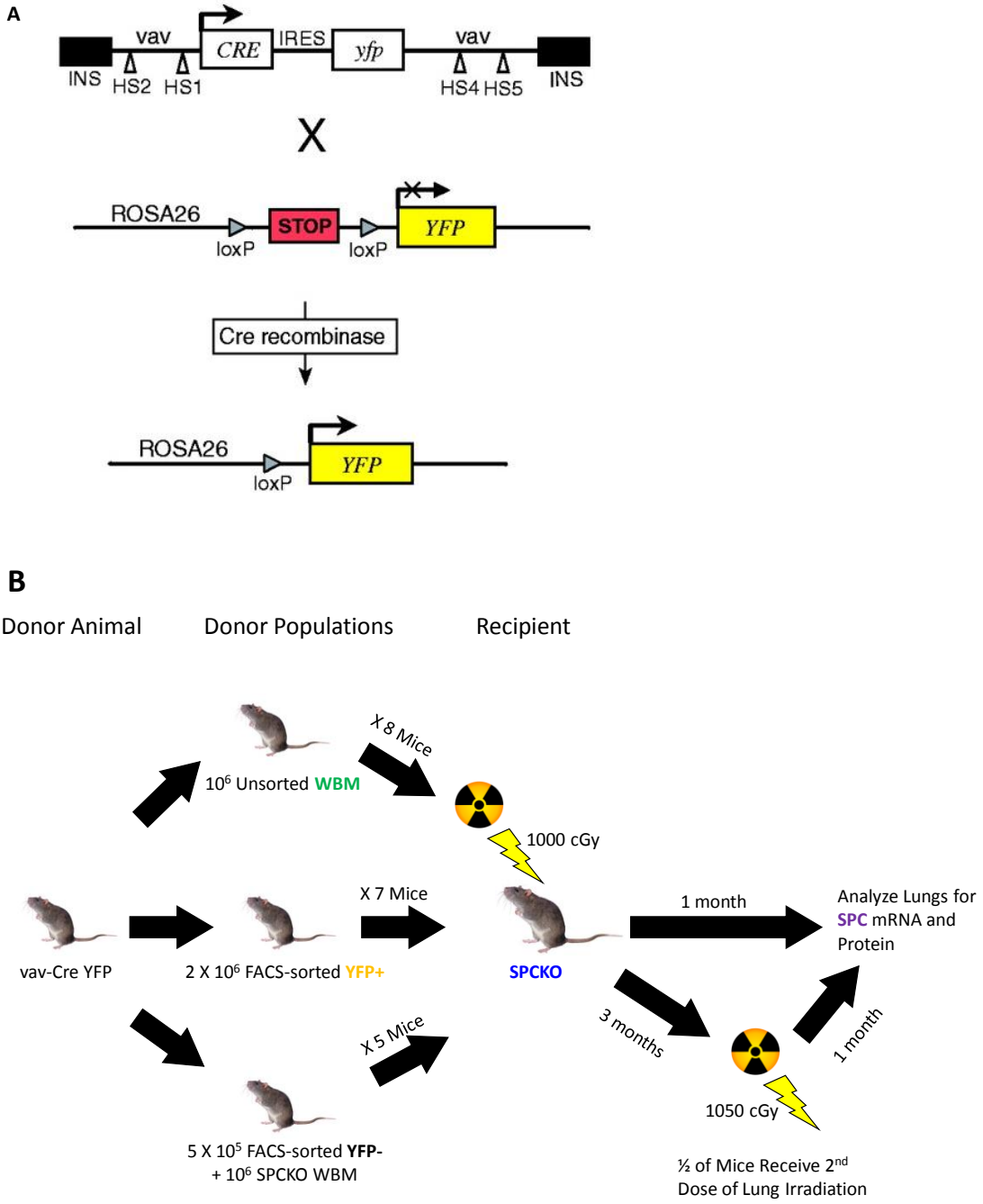

Figure 2: Schematic Showing the Experimental Design for Vav Ancestry Studies

Panel A demonstrates the genetic design of vav ancestry mice. At top, the vav-Cre bicistronic transgenic vector showing the hypersensitivity sites (HS) of the vav

elements, the insulator sequences (INS), and the IRES-YFP element which is not functional in vivo (as indicated by the lowercase letters). The middle and bottom sequences show the ROSA26R-YFP locus floxed before and after Cre-mediated excision of the stop cassette. The resultant F1 generation expresses YFP only in the hematopoietic system. Figure adapted from Stadtfeld et al (77).

Panel B presents the experimental transplantation schemes. NB The number of transplanted mice does not equal the final number of mice analyzed due to expected animal loss following irradiation.

METHODS

Transgenic Mice

SPC knockout mice (SPCKO) were obtained from the laboratory of Dr. Jeffrey Whitsett (Children's Hospital, Cincinnati, OH). These mice were generated by targeted insertion of a 5.6 kB PKG Neomycin cassette into the polyvaline region of exon 2 that gives SPC its hydrophobic functional properties. These mice completely lack mRNA by Northern blot and RT-PCR, and protein by Western blot for mature SPC and immunohistochemistry (IHC) for pro-SPC. On a 129/Sv background, this deletion confers regional emphysema and interstitial pneumonitis with respiratory insufficiency (7). Wild-type 129/SvJ mice were used as donors and controls and obtained from The Jackson Laboratory (Bar Harbor, ME).

The experiment involved with isolating engrafted type II pneumocytes by FACS utilized constitutively expressing eGFP mice under the ubiquitin-C promoter on a C57BL/6 background which were donated by Jiankan Guo (Yale University, New Haven, CT). Recipient mice were C57BL/6J-*Tyr*$^{c\text{-}2J}$/J albino mice that carry a mutation in the tyrosinase gene. This alteration results in a complete absence of pigmentation in the skin, hair, and eyes, which was irrelevant for this study (The Jackson Laboratory).

Vav ancestry mice were previously described by Stadtfeld et al (77). The details of their construction has already been presented in the Introduction,

Statement of Purpose, and Figure 2 of this work. These mice were the gift of Thomas Graf (Albert Einstein College of Medicine, New York, NY). Basically, vav ancestry mice were created by crossing vav-Cre transgenic mice with ROSA26R-YFP reporter mice. Mice with YFP+ cells of dendritic morphology were classified as vav ancestry mice. These mice were then bred for homozygosity on a C57BL/6 background by crossing female vav ancestry mice with male ROSA26R-YFP.

Stem Cell Isolations

(The FLH isolations were performed with the collaboration of Lin Wang.)

Donor animals were anesthetized using isoflurane, sacrificed by cervical dislocation, limbs removed, and bone marrow harvested by crushing the bones with mortar and pestle in 3% fetal bovine serum (FBS) in phosphate buffered saline (PBS).

Fractionated, lineage-depleted, and homed (FLH) cells were harvested using a multi-step process based on the previously described ELH technique by Krause et al (19) with slight modifications. Without a functional elutriator, harvested cells were separated based on size using a percoll gradient. The purified HSCs reside at the bottom of the 3rd fraction corresponding to a density of 1.081-1.087 g/ml. Instead of using "rotor-off" cells as previously published, short-term reconstituting radioprotection cells were provided by unfractionated whole bone marrow cells identical to the recipient.

In a summary of the following steps, these cells were then depleted of mature differentiated hematopoietic cells using immunomagnetic lineage depletion cocktail against Ter-119 for erythrocytes, CD11b for macrophages and granulocytes, CD3 for T-cells, and B220 for B-cells (BD Biosciences, San Jose, CA) as described in the BD iMag Cell Separation System protocol. The resultant population was labeled with the fluorescent tracking dye PKH26 (Sigma-Aldrich, St. Louis, MO) and transplanted into lethally irradiated (1100 cGy) recipient mice. Two days after transplantation, the bone marrow was harvested using the crushing technique from the primary recipient, and $PKH26^{+}$ cells that have homed to the bone marrow were collected by FACS. A summary of this purification is presented in Figure 3. These FLH cells are then used for further transplantation studies.

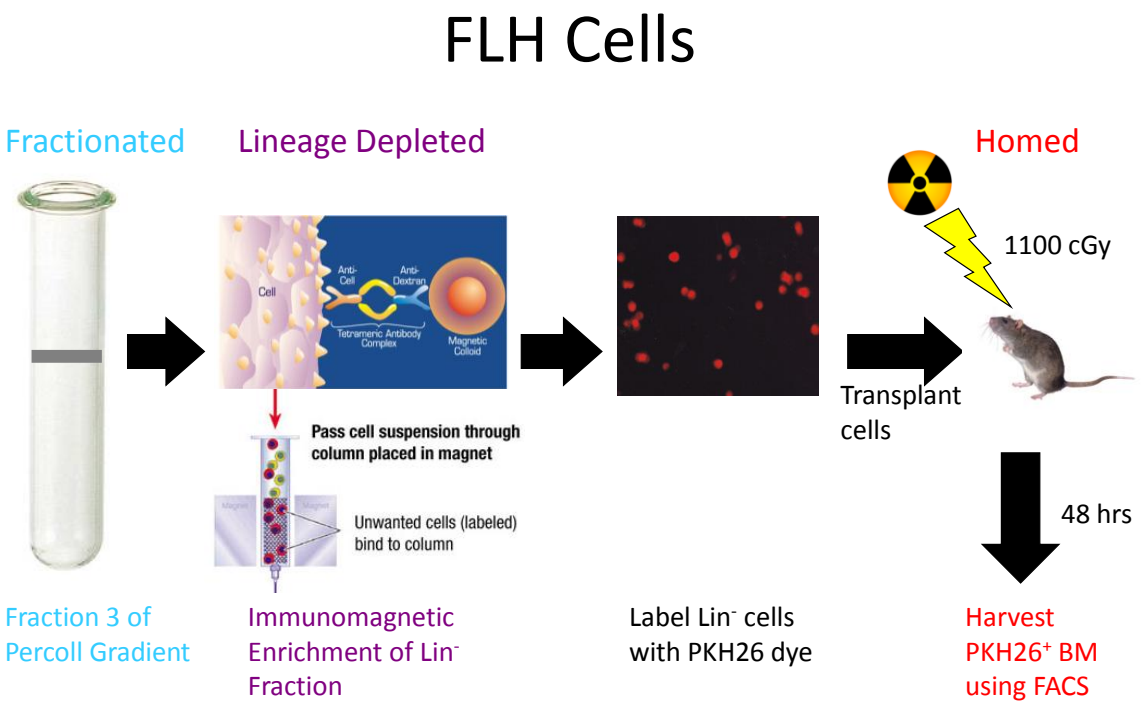

Figure 3: A Schematic Representation of the Purification of FLH cells

The LSK population and its isolation have already been well described (78). Briefly, whole bone marrow was erythrocyte lysed, lineage depleted using immunomagnetic separation (as above), and then sorted using FACS for cell surface markers. The lineage depleted cells were stained at the standard concentration of 1 µg/ 1 million cells with Sca-1 Alexa 647, c-Kit PE-Cy7, and biotinylated lineage mix PE F9 (BD Biosciences). The first gate collected living cells of appropriate size and granularity using forward and side scatter. The second gate sorts for the lineage-fraction. Finally these cells were sorted to contain the Sca-1$^+$c-Kit$^+$ fraction. A sample of the results for this sort can be seen in Figure 4.

Six week-old vav ancestry mice were sacrificed and their bone marrow harvested using the crushing technique. As with the LSK cell isolation, the whole bone marrow was then erythrocyte lysed and sorted using FACS. This time cells were stained for CD3 PE (BD Biosciences) as a marker for T cells. After forward and side scatter gating, the CD3- fraction was used in an effort to reduce T cells and the possibility of donor and recipient incompatibility. This was a remote concern since the donor mouse is on a C57BL/6 background and the recipient mice are on a 129/SvJ. Our lab's experience suggests that there is no risk of rejection or graft versus host disease, but this precaution was still taken. YFP positive and negative populations were separated using endogenous fluorescence and the resultant CD3-YFP+ and CD3-YFP- populations used for transplantation. A sample of the results of this sort can be seen in Figure 4.

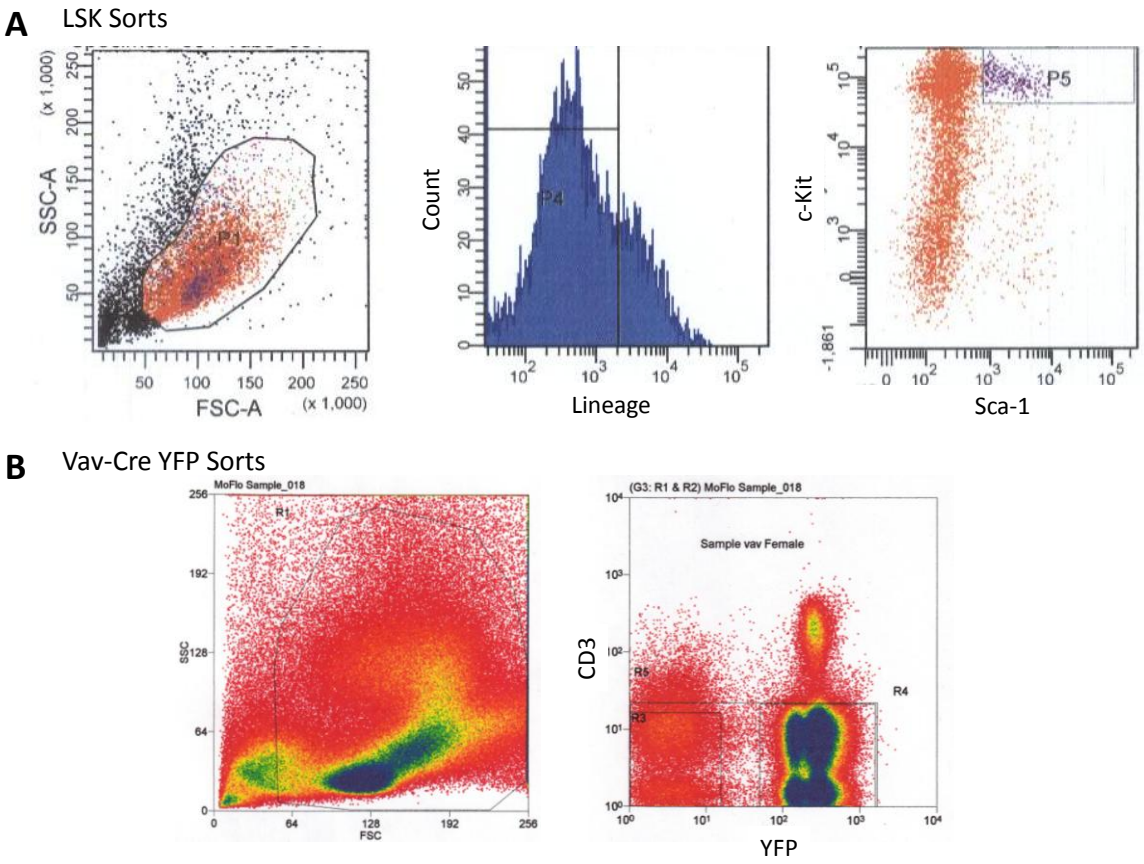

Figure 4: FACS Data Demonstrating LSK and Vav-Cre YFP Separations

Panel A contains a representative FACS plot for LSK sorts. The P1 polyhedron contains the living cells based on forward and side scatter. The P4 fraction contains the lineage negative cells. The P5 rectangle represents the final lineage$^-$Sca-1$^+$c-Kit$^+$ population which was transplanted. This population represents ~26,000 cells or about 3.4% of starting input. This was the typical yield for this population.

Panel B contains a representative FACS plot for vav-Cre YFP sorts. Again, the R1 polyhedron gates based on forward and side scatter for living cells. The R3 box contains the CD3$^-$YFP$^-$ fraction which is ~20,000 cells or about 5% of the starting input. The R4 box represents the CD3$^-$YFP$^+$ fraction which contains ~261,000 cells or about 65% of cells. Both the CD3$^-$YFP$^-$ and the CD3$^-$YFP$^+$ populations were transplanted as described in the experimental design. The R5 rectangle is used to show the entire CD3$^-$ fraction but is not relevant in this study.

Bone Marrow Transplantations

(Transplantations were performed with the assistance of Sharon Lin. The vav ancestry studies performed with the collaboration of Susannah Kassmer.)

After myeloablation with 1000-1100 cGy total body gamma irradiation using a Mark I-68A Cesium-137 Irradiator (JL Shepherd & Associates, San Fernando, CA), 6 to 8 week-old male SPCKO mice received isoflurane anesthesia and a 150 µl retro-orbital injection of transplanted cells which were resuspended in Improved Minimal Essential Medium (IMEM; Gibco) supplemented with 1X penicillin/gentamicin/streptomycin (100 µg/ml). There were 4 donor groups all of which were age-matched and sex-mismatched: 1 million unfractionated nucleated wild-type 129/SvJ WBM cells (n=5), 1 million unfractionated nucleated SPCKO WBM cells (n=5) as a transplantation control for radioprotection cells only, 1000 wild-type FLH cells along with 100,000 SPCKO WBM radioprotection cells (n=9), and 1000 wild-type LSK cells along with 100,000 SPCKO WBM radioprotection cells (n=9) (refer to Figure 1). The basics of this method have been previously described (40). Additional untransplanted controls included WT and SPCKO strains. (NB Radioprotection cells must be transplanted in order for the mice to survive the otherwise lethal dose of radiation. To reduce confounding, the number of cells transplanted was determined to be the smallest number possible such that around 50% of the animals survive. These cells are identical to the recipient and typically have a survival of less than 3 months which means that at the time of analysis they should make no contribution to the surviving animal.) Following transplantation,

the mice received sulfatrim and autoclaved food and water for 1 month, after which they received routine daily care by the Yale Animal Resources Center (YARC).

A similar method was used for the investigations involving the isolation of engrafted T2 pneumocytes using FACS sorting. Female albino 6 to 8 week-old C57BL/6 recipient mice (n=14) were irradiated with 950 cGy and then transplanted with 1 million male unsorted nucleated WBM cells from the ubiquitin-GFP^{+} mouse. Injection was performed through the tail vein and 4 unirradiated/untransplanted recipient mice were left as controls. These transplanted mice then underwent the same care as above at YARC and were sacrificed and analyzed at a 6-month time point.

The vav ancestry studies were also performed using similar methods and tail vein injection. Recipient 6 week-old SPCKO mice (n=20) were irradiated with 1000 cGy and then transplanted with one of three populations from the vav ancestry mice, which were age-matched and sex-mismatched: 10^6 vav-Cre YFP unsorted nucleated WBM cells (n=8), 2 X 10^6 FACS-sorted CD3-YFP+ cells (n=7), or 5 X 10^5 FACS-sorted CD3-YFP- cells along with 10^6 unsorted nucleated SPCKO WBM for radioprotection (n=5). (NB This last group needed supplemental SPCKO WBM cells since the YFP- population does not contain hematopoietic cells and would have otherwise died from radiation toxicity.) The unsorted vav-Cre YFP WBM population served as the control against which the sorted populations would be compared. The differing number of cells transplanted was a result of the differing values of cells yielded after FACS analysis. These transplanted mice then underwent the same care

as above in YARC. At the 1-month time point, half of these animals were sacrificed and analyzed. The other half experienced a second dose of targeted lung irradiation at the 3-month time point. One month following this treatment, this group of animals was sacrificed and analyzed.

Targeted Lung Irradiation

(Performed with assistance from Susannah Kassmer.)

Three months following transplantation of vav-Cre YFP bone marrow into SPCKO recipients (n=8), the right lung was selectively irradiated with 1050 cGy using a Siemens Stabilipan 250kV unit (Malvern, PA). Custom fit lead shields were used to localize the dose of radiation.

Mouse Sacrifice and Lung Tissue Harvest

Mice were sacrificed at 3 months post-transplantation unless stated otherwise. Mice were anesthetized with urethane IP injection and bronchoalveolar lavage with 2 ml of PBS was performed using a 23G angiocatheter (Becton-Dickinson, Franklin Lakes, NJ) into the trachea. Then right ventricular perfusion was performed using the standard method of a median sternotomy approach such that the right heart is punctured with a 23g needle and flushed with 10 ml of PBS into the pulmonary circulation. The lungs were then inflated with 1 ml of 1% low melt

agarose in PBS at 42°C through the angiocatheter in the cannulated trachea. The agarose was then allowed to cool and solidify over a couple of minutes.

Tissue Fixation and Cytospin Preparation

The murine right lung was placed into 4% buffered formalin for 4 hours and then transferred to 70% ethanol prior to paraffin embedding and sectioning. The left lung was divided into 2 pieces based on lobe segments. One piece was placed into RNAlater stabilization reagent (Qiagen, Valencia, CA) and frozen in -80°C per manufacturer's recommendations for later use in RNA isolation. The other piece was used for single cell lung digestion, immunodepletion, and cytospins.

This preparation involved multiple modifications from the originally described procedure by Corti et al (79). The resulting lung piece was minced with a fresh razor blade then digested for 90 minutes at 37°C using a fresh 5 ml solution of Dulbecco's Modified Eagle Medium (DMEM, Gibco, Invitrogen) supplemented with dispase (2.4 U/ml, Roche), collagenase (133 U/ml Worthington Biochemical Corporation, Lakewood, NJ), and DNAseI (100 U/ml, Roche). The digested tissue was then ground through a 40 micron strainer (Falcon, Oxnard, CA) and the filter flushed with an additional 5 ml of DMEM. The cells were centrifuged at 800g for 10 minutes and the supernatant removed. In order to remove erythrocytes, 2 ml of 1X Pharmlyse (Pharmingen, San Diego, CA) was added for 5 minutes at room temperature (RT) per the manufacturer's instructions. The cells were then washed

in PBS, counted, and resuspended in 3 ml of PBS supplemented with 3% BSA and 5mM EDTA at 1,000,000 cells per ml.

The concentrated and digested lung cells were then immunodepleted using magnetic bead separation per manufacturer's protocol (BD Biosciences). Anti-mouse CD45 and anti-mouse CD11b biotinylated antibodies (1µg/million cells) were added to the cells and mixed so as to remove hematopoietic cells and macrophages from the digestion. This mix was incubated at RT for 15 minutes then streptavidin magnetic beads (5µl/million cells) were added and the entire solution refrigerated at 4°C for 30 minutes. The contents were then placed in the BD iMagnet for 8 minutes after which the $CD45^{-}CD11b^{-}$ supernatant was removed and the cells were counted.

The immunodepleted cells were then spun (20,000 cells/slide) onto Surgipath (Richmond, IL) precleaned slides in a Thermo-Shandon cytospin (Pittsburgh, PA) at 700 rpm for 7 minutes after which they were fixed in 4% paraformaldehyde (PFA) for 15 minutes. The slides were rinsed with dH_2O and air dried at RT for at least 1 hour prior to storage at -80°C. From the starting population of approximately 2 million lung cells per animal, typically greater than 300,000 cells remained following immunodepletion.

Immunofluorescence on Paraffin Sections and Cytospins

Slides were deparaffinized with heat at 60°C and washed with Citrisolve. They were then rehydrated using successive ethanol baths of 100%, 95%, and 70%. Following a brief wash with PBS, the sections underwent an antigen retrieval step if necessary. This involved adding boiling BD Retrievagen citrate pH 6 solution (BD Pharmingen, San Diego, CA) to the slides in coplin jars. The slides were then kept in a steamer for 30 minutes and allowed to cool to RT, followed by a wash in 1X PBS with 0.25% Triton-X for 10 minutes. The slides were blocked with 3% BSA in 1X PBS with 0.25% Triton for 1 hour in a moisture chamber at RT and then incubated overnight at 4°C with the primary antibody mix under a coverslip to localize the antibodies and avoid evaporation. The primary antibody mix included either polyclonal guinea pig α mouse SPC 1:1000 (courtesy of Jeffrey Whitsett) or polyclonal rabbit α mouse pro-SPC 1:50 (Chemicon, Millipore, Billerica, MA). Additionally, the mix contained rat α mouse CD45 and F4/80 in a 1:50 dilution (both from Abcam, Cambridge, MA). Following a washing step with PBS/Triton, secondary antibody mix of either α guinea pig or α rabbit AF488 at 1:500 and α rat AF 547 at 1:250 in blocking buffer was added for 1 hour at RT. The slides were again washed and mounted with VECTASHIELD containing DAPI (Vector Labs, Burlingame, CA, USA).

Cytospin slides were thawed to RT and permeabilized with PBS/Triton before primary antibody mix was added. The subsequent steps were the same as for the above paraffin section protocol. Antigen retrieval was never used on these slides.

Microscopy

(Confocal work completed with the collaboration of Susannah Kassmer.)

Light microscopy was performed on an Olympus BX51 microscope equipped with a Sensicam^{QE} camera. IPLAB software was used to capture images. Confocal microscopy images were obtained on a Leica TCS SP5 Confocal Microscope equipped with 405 Diode, Argon, Helium/Neon 543, and Helium/Neon 633 lasers. These images were collected and analyzed by Leica LAS AF software. Confocal microscopy with 3-dimensional z-stack analysis was used to reimage these cells. All microscopic analyses were performed with the investigator blinded regarding the identity of the slides analyzed.

RNA Isolation and Quantitative Real-Time PCR

All tools and surfaces were either autoclaved with diethylpyrocarbonate (DEPC) water or treated with RNase Zap (Ambion, Austin, TX) prior to usage. Total RNA was extracted from approximately 30 mg of lung tissue which was previously stored in RNAlater. The RNeasy Mini kit (Qiagen) was used per manufacturer's recommendations with the addition of an RNase-free DNase I (Qiagen) digestion step to eliminate genomic DNA. The resultant RNA was qualified and quantified using the NanoDrop ND1000 Spectrophotometer (Thermo Scientific, Wilmington, DE), and then reverse transcribed using Superscript II Reverse Transcriptase (Invitrogen) and random hexamer primers (Invitrogen) to create cDNA.

Quantitative real-time PCR was performed using a BioRad CFX96 Real Time System (Hercules, CA). Amplification was performed for 40 cycles (10 seconds denaturation at 95°C, 30 seconds annealing at 60°C, and 30 seconds elongation at 72°C) using approximately 200 ng of cDNA in a SYBR green master mix (Applied Biosystems) as directed. All reactions were performed in triplicate and any samples that were greater than 1 cycle difference in their threshold calculation (termed C(t)) were repeated. Primer for ribosomal 18s or β2-microglobulin was used as the internal control for total RNA content. All reactions included non-template controls, non-reverse transcriptase controls for DNA contamination, WT positive control, and SPCKO negative controls.

SPC primers spanned the disrupted exon 2 insertion site to the end of the full length mRNA and were designed as follows: Fwd 5'-ATG GAG AGT CCA CCG GAT TAC-3' and Rev 5'-ACA GAC TTC CAC CGG TTT CTG-3'. These primers amplify a 664 base pair fragment. 18s rRNA primers were designed as follows: Fwd 5'-CGG CTA CCA CAT CCA AGG AA-3' and Rev 5'-GCT GGA ATT ACC GCG GCT-3'. β2-microglobulin primers were designed as follows: Fwd 5'-CAT ACG CCT GCA GAG TTA AGC A -3' and Rev 5'- GAT CAC ATG TCT CGA TCC CAG TAG-3'. All primers had a melting temperature of 58-62°C. The difference in cycle threshold (termed Delta C(t)) was calculated by subtracting the mean C(t) of 18s or β2 by the mean C(t) of SPC for each individual sample. Statistical significance between groups was confirmed at p-values less than 0.05 and calculated using the 1 tailed, homoscedastic, t-test .

FISH For Y-Chromosome

To determine levels of hematopoietic engraftment, blood smears and bone marrow cytospins from sacrificed mice were prepared and fixed in formalin as described above. The slides were washed with PBS, and Y-probe (developed by degenerate oligonucleotide primed-PCR using 6AI primer = 5'-CCG ACT CGA GNN NNN NTA CAC C-3' supplied by Lin Wang, Yale University) was added to heated slides at 60°C and incubated overnight at 37°C. Following washes with 2X SSC, slides were blocked with 4xSSC/3%BSA/0.1%Tween-20 for 30 min at 37°C, washed again, and stained with anti DIG-rhodamine (Roche, Mannheim, Germany) at 1:10 in blocking buffer for 45 minutes at 37°C . The detection solution was washed away and the slides were mounted with VECTASHIELD including DAPI.

Fluorescence Activated Cell Sorting Analyses

All FACS sorts were performed on either a BD FACSAria Special Order System or MoFlo XDP Cell Sorter (Beckman Coulter, Brea, CA). FACS data was analyzed with FlowJo 8 Analysis Software (Ashland, OR). Regarding the GFP^+ into wild type transplantations, engrafted donor-derived T2 lung cells were described as $GFP^+CD45^-CD11b^-CD31^-$ and these cells were sorted onto a poly-L-lysine coated glass bottom dish containing DMEM supplemented with 3% FBS and 1X penicillin/streptomycin. The sorted cells were allowed to attach to the plate overnight at 37°C and subsequently fixed with 4% PFA before being examined by immunofluorescence as above.

RESULTS

Establishing and Validating Methods

Before our experimental investigations, we had to determine that our method of detecting target genes was satisfactory. In particular, we were concerned with the sensitivity and specificity of immuno-staining for SPC in both paraffin-fixed sections and single cell suspensions on cytospins. Wild-type mice (WT) lungs were used as the positive control while knockout mice for SPC (SPCKO) lungs served as the negative control. Various preparation techniques were utilized with or without antigen retrieval. Additionally, two different antibodies (guinea pig-raised polyclonal and rabbit-raised polyclonal, refer to Methods for details) were used to assess the clearest staining with the least amount of background. The comparison of these stainings in paraffin sections can be seen in Figure 5. As expected, the SPC staining pattern was vesicular in nature and located in the cytoplasm. The brightest staining for SPC in WT mice was observed using the guinea pig-derived antibody without the use of antigen retrieval. This finding coupled with the lack of significant background fluorescence seen in SPCKO mice made this combination most desirable for future investigations, and determined that in our hands SPC positive T2 cells could be detected.

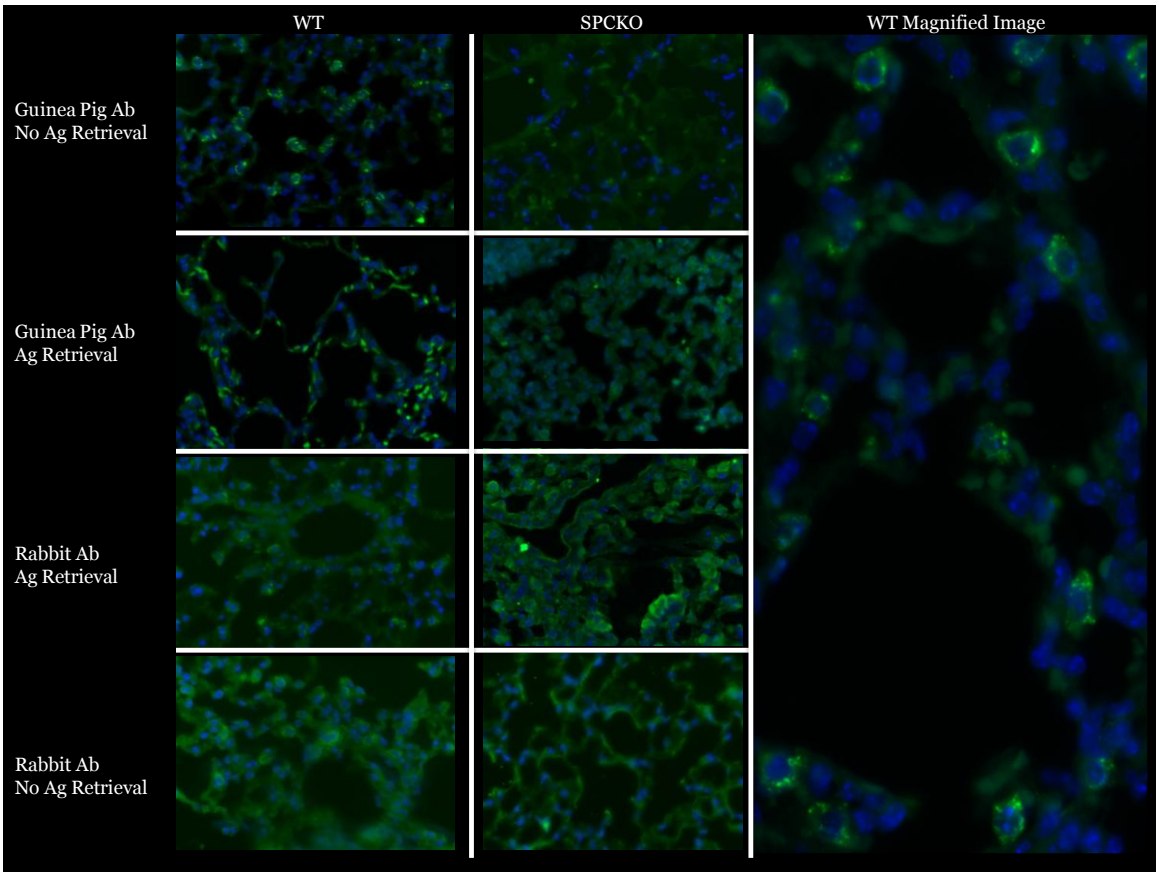

Figure 5: A Comparison of SPC Staining Protocols for Mouse Lungs

Four different combinations of antibodies and slide preparations are shown here. WT images (in left panels) represent the positive control for SPC staining whereas SPCKO is the negative control (in middle panels). Guinea pig antibody without an antigen retrieval step seemed to yield the best results with definitively SPC-positive cells in the WT and a low amount of background in the SPCKO. A magnified image of the WT lung is shown to demonstrate the vesicular nature of SPC staining (right panel). Staining: DAPI (blue) for nuclei, SPC (green) for T2 pneumocytes. Images were produced using light microscopy on 40X objective magnification.

Single cell digested cytospin stainings were also optimized in the same manner as paraffin sections. Since these original lung digestions were unsorted (i.e., there was no lineage depletion step for contaminating blood cells) and T2 cell morphology is lost during digestion, CD45 (a pan hematopoietic cell surface marker) and F4/80 (a macrophage marker) staining antibodies were included. This additional staining was of particular importance in recognizing macrophages, which are known to show spurious SPC staining and mimic T2 pneumocytes, either due to invagination of SPC in vivo or due to autofluorescence. Positive CD45 and F4/80 staining is typically diffusely distributed throughout the cell membrane and this pattern was observed in many of the cells on these slides. Type II cells were $SPC^{+}CD45^{-}F4/80^{-}$ which would make them appear green only; whereas macrophages were either $SPC^{-}CD45^{+}F4/80^{+}$ or $SPC^{+}CD45^{+}F4/80^{+}$ resulting in a red or yellow color, respectively, on multi-color merged images. Upon examination, the same combination of guinea pig-derived antibody with no antigen retrieval resulted in the clearest cytospin data as seen in Figure 6. These cytospins provided excellent visualization of the WT positive controls and the SPCKO negative controls; however the rarity of BMDC in the next experiments will necessitate an additional selection step to enrich for T2 cells.

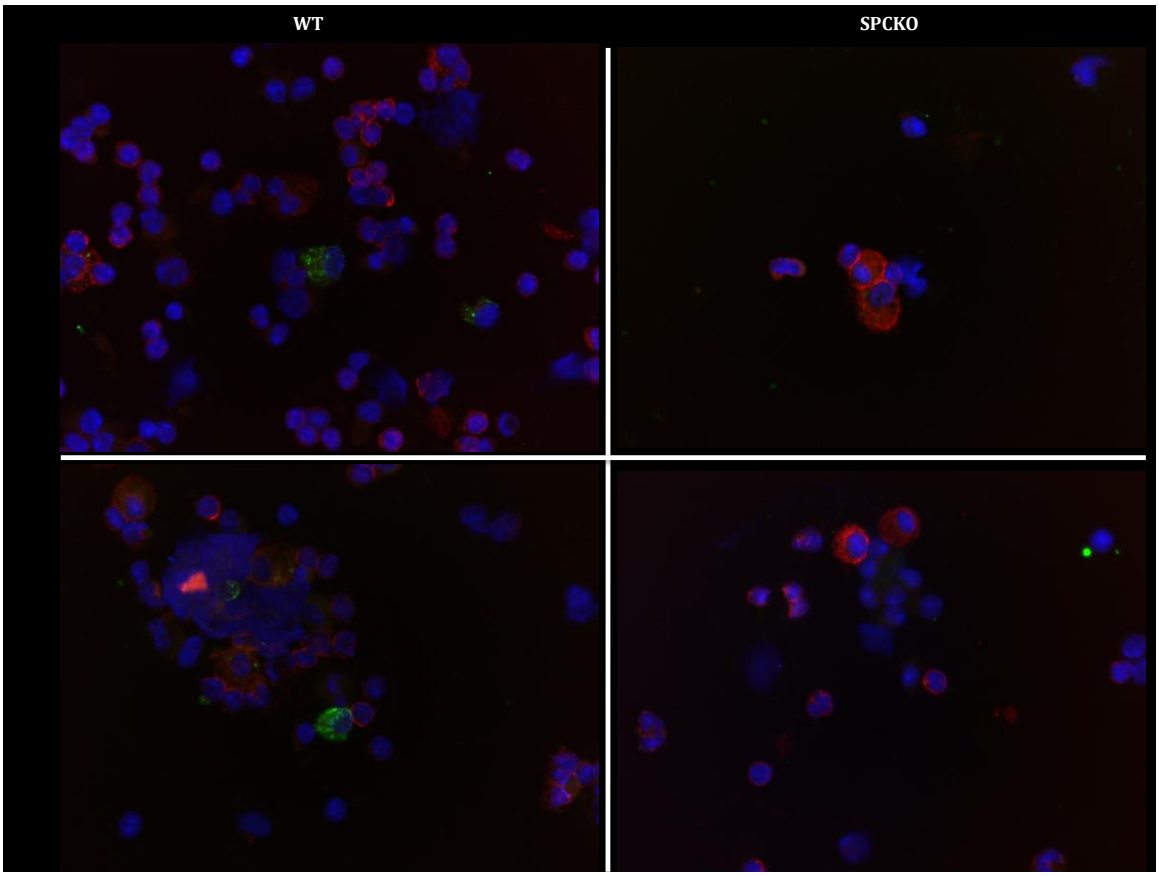

Figure 6: Successful SPC, CD45, and F4/80 Staining of Lung Cytospins

Two examples of clear staining with SPC, CD45, and F4/80 using positive (WT in left panels) and negative (SPCKO in right panels) control slides. The WT slides contained many $SPC^{+}CD45^{-}F4/80^{-}$ cells, which are T2 pneumocytes while the knockout slides did not have any SPC^{+} cells. Many blood and tissue macrophages can be seen in these images as $CD45^{+}F4/80^{+}$. These results validated that our detection techniques will be sufficient moving forward. Staining: DAPI (blue), SPC (green), CD45 (red), and F4/80 (red). Images were produced using light microscopy on 40X objective magnification.

BMDCs Can Engraft In the Lung As Type II Pneumocytes

As a re-exploration of previously published data with newer more rigorous methods, we attempted to determine if BMDC could engraft as T2 pneumocytes in the lungs of transplanted mice. Following lethal irradiation of 1000cGy and transplantation of 10^6 WT WBM cells, the recipient mice were evaluated for lung epithelial engraftment three months later. SPC was used as a marker for donor-derived cells since the donor mice were wild type for SPC while the recipients were SPC knockouts. Also included in the study were WT and SPCKO untransplanted controls along with a transplantation control of SPCKO into SPCKO (refer to Figure 1 for more details).

In almost 25% of the WT into SPCKO transplants, BMD T2 pneumocytes could be detected using immunofluorescence (refer to Table 2). These cells were $SPC^+CD45^-F4/80^-$ in either paraffin or cytospin sections. It should be noted that these single cell digestion cytospins were red blood cell lysed as well as immunodepleted using CD45 and CD11b (macrophage/monocyte specific marker). This greatly enhanced our ability to find epithelial cells of the lung parenchyma. The typical appearance of these cells is shown in Figure 7. Unfortunately, the number of BMD T2 pneumocytes in any given animal was exceedingly small. The number of cells ranged from 1-3 per 5 micron section which contained approximately 70,000 nucleated cells. As a point of reference, for WT mice about 20% of nucleated alveolar epithelial cells and 7.91% of total DAPI nuclei were SPC positive, which is consistent with previously published results (80).

Mouse Type	N	Number of Mice with $SPC^+CD45^-F4/80^-$ Cells	Percentage of Mice with $SPC^+CD45^-F4/80^-$ Cells	Mean Percentage of Cells that were SPC^+
WT→SPCKO	21	5	24%	0.002%
SPCKO→SPCKO	5	0	0%	0.000%
WT Control	5	5	100%	7.91%
SPCKO Control	5	0	0%	0.000%

Table 2: BMD Type II Pneumocytes Can Be Seen In WBM Transplants

Using immunofluorescence on either paraffin sections or immunodepleted cytospin slides, 24% of mice transplanted with WBM were able to demonstrate at least a very low level of epithelial engraftment as T2 pneumocytes. The level of engraftment was quantified to be approximately 0.002% of T2 cells based on SPC immunostaining compared to 0.000% in both the transplantation SPCKO→SPCKO negative control and 0.000% in the untransplanted SPCKO negative control.

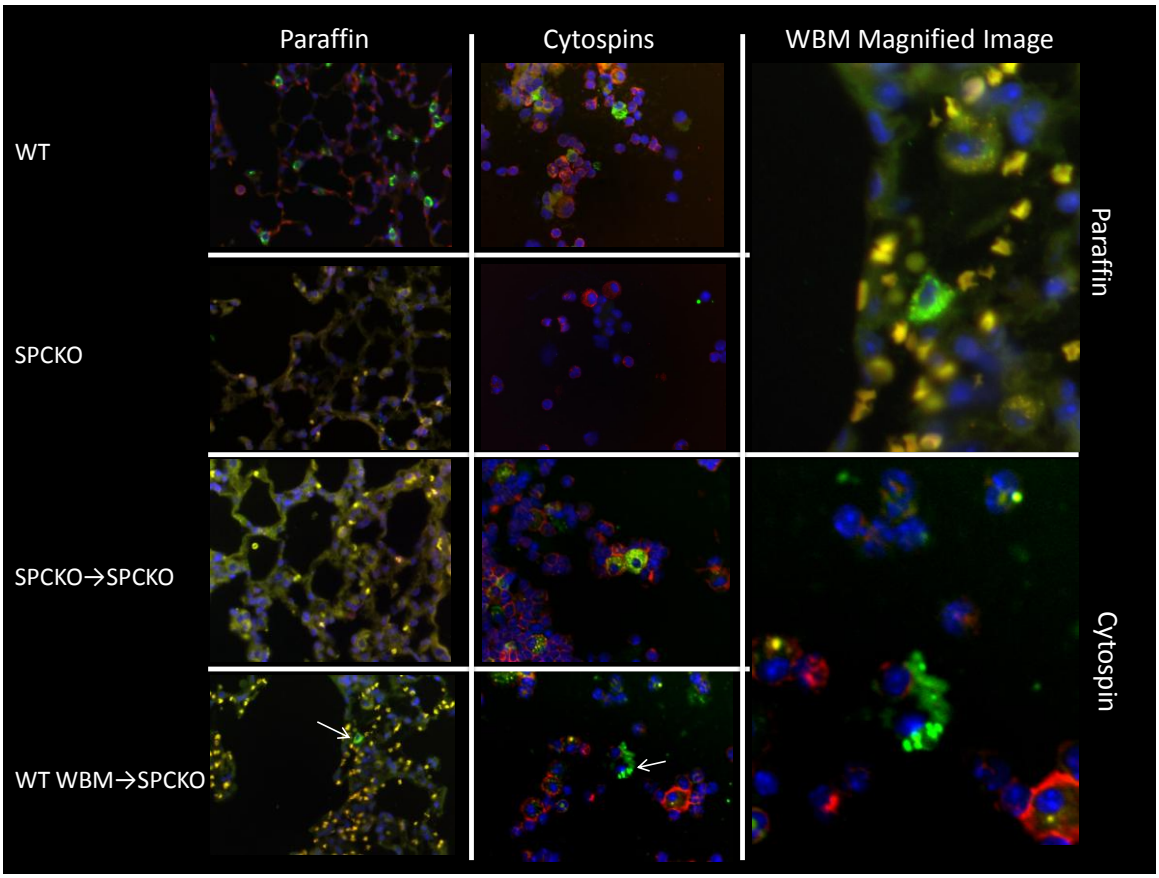

Figure 7: Sample Paraffin and Cytospin Sections Demonstrating Engraftment

Paraffin sections (left panels) and cytospins (center panels) demonstrating rare $SPC^{+}CD45^{-}F4/80^{-}$ cells suggestive of a donor-derived T2 cell (arrows). WT image represents the untransplanted positive control. SPCKO is the untransplanted negative control. SPCKO→SPCKO is the transplantation control of radioprotection SPCKO WBM cells only. High magnification images of the WBM transplants (right panels) are also shown to demonstrate the vesicular nature of SPC staining. Staining: DAPI (blue), SPC (green). Antibodies against CD45 (red) and F4/80 (red) for hematopoietic cells and macrophages, respectively, were included to indicate blood cells. Yellow cells are autofluorescent erythrocytes and macrophages. Images were produced using light microscopy on 40X objective magnification.

FLH and LSK Transplants Engraft in The Lung

Based on current available evidence, it is not clear if purified bone marrow cells offer an engraftment advantage in the lung compared to whole bone marrow. We therefore sought to answer this question using two well described populations which are known to be enriched for HSCs. Unfortunately, ELH cells could not be isolated due to a non-functional elutriator. However, a percoll fractionation technique has been shown to yield a theoretically similar subpopulation as the elutriation separation (81). These cells were therefore referred to as fractionated, lineage-depleted, and homed (FLH). Like ELH cells, FLH cells were shown to home to the bone marrow and provide long-term hematopoietic reconstitution. However, it remains an open question if FLH cells are truly identical to ELH cells. The second purified population studied was the well defined LSK group which is separated by FACS using cell surface markers. Utilizing a similar method as before, mice were lethally irradiated with 1000cGy and then transplanted and evaluated for lung epithelial engraftment three months later. The only difference in the methods was that 10^3 FLH or LSK cells derived from WT mice were transplanted along with 10^5 radioprotection cells (which are short term reconstituting WBM cells identical to the recipient SPCKO). These radioprotection cells are necessary for animal survival following irradiation and have a lifespan maximum of 3 months. Therefore at the time of analysis these cells should have minimal influence on engraftment.

Sex-mismatched transplants were done (i.e., female BMDC into male recipients) so that hematopoietic engraftment could be assessed at sacrifice using Y-FISH on peripheral blood smears or bone marrow cytospins. Positive (male) and

negative (female) controls showed >99% and <1% Y-chromosome positive cells respectively. When this blood chimerism was examined 1 month post-transplant, 3 of 5 animals transplanted with FLH cells and 3 of 5 animals transplanted with LSK cells showed greater than 5% chimerism (refer to Table 3). As controls, 4 of 4 animals that received WT WBM and 4 of 5 animals that received SPCKO WBM had significant levels of hematopoietic engraftment. These quantifications were based on counting a minimum of 100 nucleated cells per slide. The greater levels of engraftment in the control groups correlated with the larger number of donor cells administered during transplantation. As suggested in the literature, despite the small numbers of animals in this study, it appeared that both FLH and LSK populations were equally capable of reconstituting the hematopoietic system. Although there was not a clear correlation between blood chimerism and identification of marrow-derived pneumocytes, the two animals that demonstrated the highest level of hematopoietic chimerism were also the only two animals to have donor derived cells on both paraffin and cytospin sections.

When examining the paraffin and cytospin sections of the lung using immunofluorescence for SPC, BMD T2 alveolar cells could be detected in both FLH and LSK transplantation groups (Table 3). In fact, 4 of 5 mice in the FLH group and 5 of 5 in the LSK group had at least 1 positive cell in either of the sections. In comparison, 2 of 4 mice in the positive control WT WBM group and 0 of 4 in the negative control SPCKO WBM→SPCKO contained at least 1 positive cell. Therefore FLH and LSK cells types show a slight enrichment for engraftment when compared to controls. It should be noted that the positive control WT WBM cytospins were

unavailable and therefore epithelial engraftment rates are likely higher than 50% if all the sections could be analyzed. Taking this into account, the data suggest that the LSK and FLH populations engraft at least as well as WBM.

Despite these promising results, it should be noted that no greater than 2 BMD T2 cells were observed on any one slide. Thus, these conversion events occurred in most animals but they were very rare. Surprisingly, there was no pattern between positive cytospin and positive paraffin results. Animals which were positive in one cell preparation type were not positive in the other except in the 2 instances explained above with the FLH mice showing the highest levels of hematopoietic engraftment. It is particularly unusual that there was no overlap in the LSK group. Beyond this, the number of positive cells seen in any one animal was never greater than 3. Sample images of positive BMD T2 pneumocytes from the FLH and LSK transplants are presented in Figure 8.

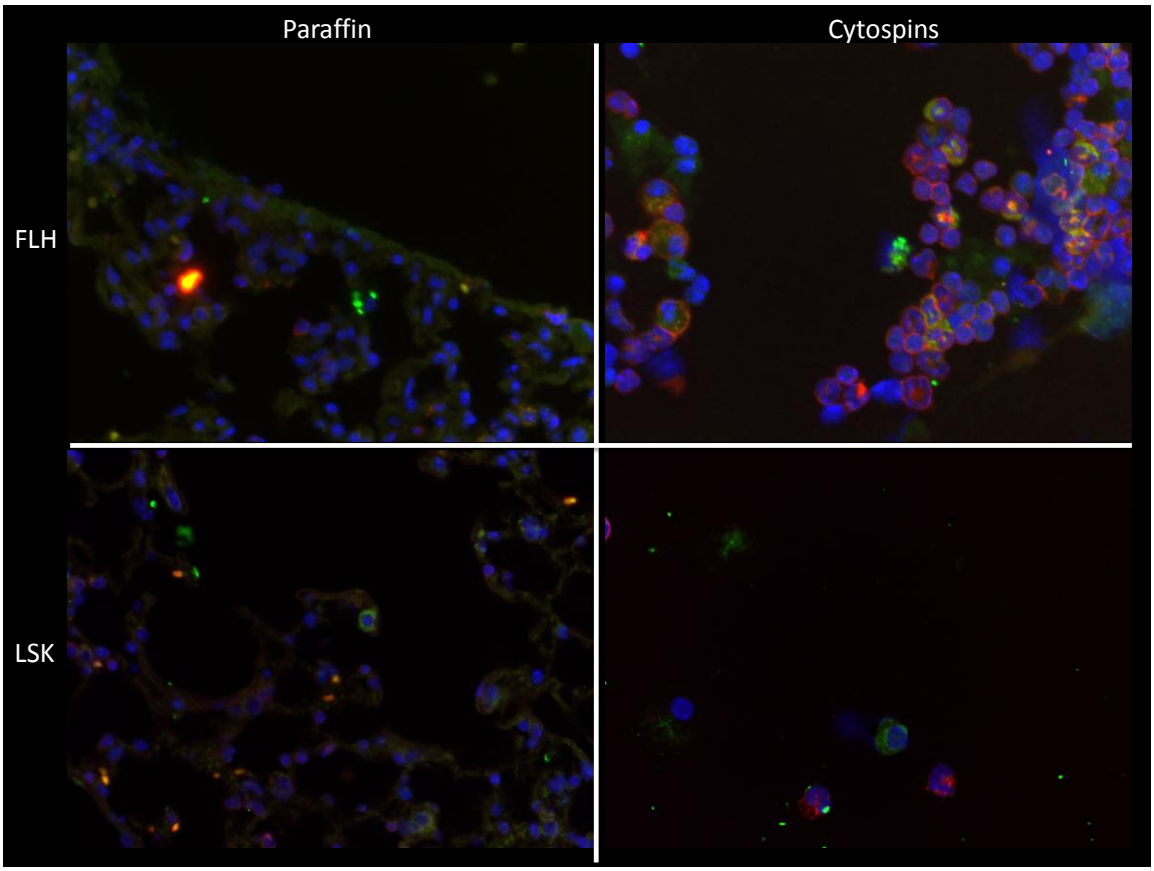

Figure 8: Representative Paraffin and Cytospin Sections from FLH and LSK Transplants Show Engraftment in the Lung

These rare BMD engrafted cells appeared similar to the untransplanted positive control WT type II pneumocytes. Staining: DAPI (blue), SPC (green), CD45 (red), and F4/80 (red). Images were produced using light microscopy on 40X objective magnification.

Quantitative PCR for SPC Shows Insignificant Increases Following Transplantation of BMDCs

To further assess engraftment of BMDC and subsequent transformation of phenotype, quantitative PCR (qPCR) for SPC was used as a very sensitive marker for functional T2 cells. Following sacrifice, total RNA from the mouse lung was isolated and then reverse transcribed into cDNA. This total lung cDNA was then assessed for

the quantity of SPC transcripts and normalized to total genetic content using 18s rRNA as the standard. Since only donor-derived cells have a functional SPC gene, any signal for SPC must have originated from these cells. qPCR is very susceptible to inconsistent results based on even minute changes in the quantity and quality of template so three control groups were used and all amplifications were performed in triplicate. WT served as the positive control and maximal amount of SPC while SPCKO was the negative control and the minimal amount of SPC. A group of SPCKO WBM cells into SPCKO mice was included to act as a negative control for irradiation and transplantation itself.

WBM and LSK transplants did not show a significant difference in the level of SPC RNA when compared to SPCKO. Interestingly and unexpectedly, SPCKO→SPCKO control and FLH populations demonstrated a greater amount of SPC RNA on the order of 100 to 200-fold, respectively. However, it is unclear how the SPCKO→SPCKO group had higher levels of SPC since the transplanted cells were SPCKO. Since the difference in SPC RNA was not significant ($p=0.38$) between the negative control SPCKO→SPCKO group and the FLH group, it was determined that no considerable amount of engrafted BMD T2 cells could be detected.

Upon further review of the project design, the FLH and SPCKO→SPCKO transplantations were performed on the same day in parallel. Therefore, this unexpected data could be the consequence of cross-contamination of WT FLH populations into SPCKO WBM animals resulting in a spuriously high qPCR signal in

the SPCKO→SPCKO group. Alternatively, there could also have been cross-contamination during RNA preparation but this explanation is less likely.

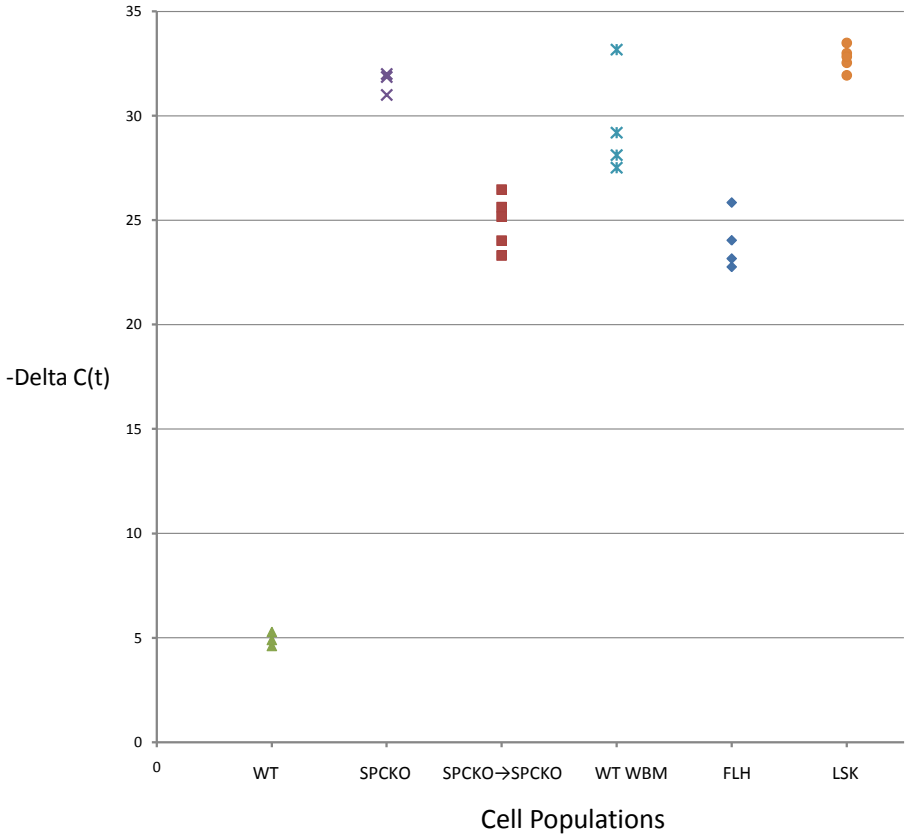

Figure 9: qPCR for SPC Demonstrating No Significant Difference in mRNA Levels Between Negative Controls and Transplanted Populations.

Even though the FLH population showed the greatest reconstitution of SPC signal it was not significantly higher than the SPCKO WBM→SPCKO negative transplantation control (p=0.38). Therefore, engraftment of BMD T2 cells could not be detected using these methods. Lower –Delta C(t) levels represent more mRNA transcripts. WT is the untransplanted positive control showing normal levels of SPC transcripts and SPCKO is the untransplanted negative control showing no SPC. Total RNA content normalized to 18s rRNA standard. Each dot represents 1 animal with the qPCR performed in triplicate.

Type	Number	% Chimerism by Y-FISH	Cytospin	Paraffin	qPCR -Delta C(t)
FLH	877	1.55 (Blood)	Negative	Positive	22.77
FLH	878	3.13 (Blood)	Negative	Negative	25.84
FLH*	884	46.88 (Blood)	Positive	Positive	31.47
FLH	892	16.67 (Blood)	Negative	Positive	23.17
FLH	893	48.67 (Blood)	Positive	Positive	24.04
LSK	1028	10.17 (BM)	Positive	Negative	31.93
LSK	1029	16.13 (BM)	Negative	Positive	32.54
LSK	1035	6.76 (BM)	Positive	Negative	32.99
LSK	1044	2.78 (BM)	Negative	Positive	32.83
LSK	1054	3.73 (BM)	Positive	Negative	33.49
SPCKO	876	4.63 (BM)	Negative	Negative	24.03
SPCKO	879	8.93 (BM)	Negative	Negative	23.30
SPCKO	880	26.92 (BM)	Negative	Negative	25.63
SPCKO	890	5.13 (BM)	Negative	Negative	26.47
SPCKO	891	Positive (BM)	Negative	Negative	25.17
WBM	M35	Positive (BM)	Unknown	Positive	27.51
WBM	M38	Positive (BM)	Unknown	Negative	28.11
WBM	M40	Positive (BM)	Unknown	Positive	29.20
WBM	1014	5.92 (BM)	Negative	Negative	33.16

Table 3: Summary of All Mice Transplanted for HSC Plasticity Studies

This table presents an overview of the data from each mouse transplanted in this experimental study. "Type" refers to the population of donor cells transplanted for this group. SPCKO is the transplantation negative control of SPCKO WBM while WBM is the transplantation positive control of WT WBM. "Number" is the animal identifier. Hematopoietic chimerism is shown as a percentage except where the specifics of this data were unavailable. The source of cells for Y-FISH analyses is shown in parentheses. Cytospin and paraffin sections of each mouse's lung were quantified as "positive" if donor-derived T2 cells could be identified and "negative" if no cells could be found. Some data were unavailable and therefore described as unknown. The final column shows the raw qPCR data for SPC. *This mouse was sacrificed at an earlier time point and its qPCR data was not consistent with the other animals in its group but it is still presented here for completeness.

FACS Sorting Allows Isolation of Rare Donor-Derived Type II Cells

Based on the rarity and difficulty of identifying engrafted T2 cells in paraffin sections and cytospins, we sought a different method to search for these events. Therefore, we investigated whether FACS analysis of the whole digested lung would be able to separate the cells of interest and allow further investigations on this rare population of transformed cells. Using a constitutively active GFP reporter mouse as a donor, 10^6 WBM cells were transplanted into a lethally irradiated wild type recipient. At six months post-transplant, the mice were sacrificed and their lungs digested in the usual fashion with erythrocyte lysis but no other methods of immunodepletion. In order to isolate donor-derived lung epithelial cells, we had to gate for GFP+ cells as well as eliminate contaminating populations. In particular, cells that have high levels of expression of CD45, CD11b, and CD31 (a surface marker specific for endothelial cells) were excluded.

The results of this FACS analysis showing 10^6 events can be seen in Figure 10. A WT mouse represents the negative control for GFP expression and the positive control for total lung epithelial cells. A constitutively GFP-expressing mouse serves as the positive control for GFP staining. The GFP transplanted mice showed a nearly 100-fold increase of $GFP^+CD45^-CD11b^-CD31^-$ cells (0.29%) over background as represented by the WT mouse (3.5×10^{-3} %). This transplanted population represented 27% of the theoretical maximum of 1.06% seen in the GFP mouse. Additionally, a comparable number of total epithelial lung cells were seen in all three mice (24.5%-32.7%). These data demonstrated that we can successfully

separate and enrich our target population for BMD lung epithelial cells using FACS analysis.

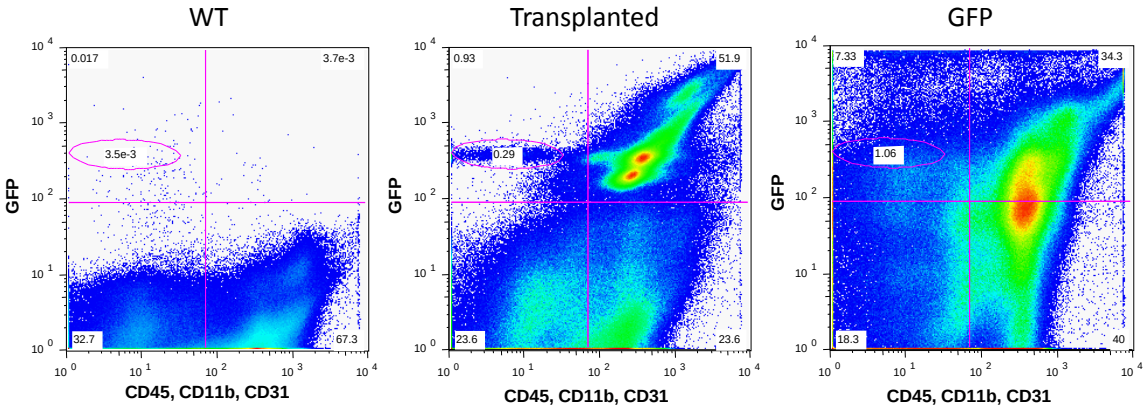

Figure 10: FACS Data Demonstrating 100-Fold Enrichment of GFP$^+$CD45$^-$ CD11b$^-$CD31$^-$ Fraction Containing BMD Lung Epithelial Cells Over Background Levels

FACS data from one million lung cells showing GFP (Y-axis) and CD45/CD11b/CD31 (X-axis) fluorescence. These data were the clearest of four GFP into WT sorts which utilized 10 animals. The target population (GFP$^+$CD45$^-$CD11b$^-$CD31$^-$) is in the oval with quantification. There is an approximately 100-fold enrichment when sorting for lung epithelial cells compared to background as represented by the WT mouse. About 27% of maximal target population can be isolated using this method. These data show that BMD lung epithelial cells can be successfully isolated in significant numbers using FACS as seen by the clear finger-like projection in the center panel. "WT" (left panel) represents the untransplanted negative control for GFP staining. "Transplanted" (center panel) represents the experimental set of GFP-expressing WBM transplanted into a wild type recipient. "GFP" (right panel) is the untransplanted positive control for GFP staining.

Imaging of FACS-Sorted Populations Confirms Lung Engraftment

Following the isolation of lung epithelial cells using FACS, we next sought to query these cells' phenotype using immunofluorescence microscopy. An additional FACS sort was performed using five WT mice that were lethally irradiated and then given 10^6 ubiquitin-C GFP WBM cells. As expected, these five mouse lungs yielded approximately 10 million total cells. The resulting $GFP^+CD45^-CD11b^-CD31^-$ fraction from these transplants was 50,000 cells (0.5%) compared to 289,000 $GFP^+CD45^-CD11b^-CD31^-$ cells out of 4 million total cells (7.2%) for the unirradiated GFP^+ positive control. The 50,000 cells were plated onto poly-L-lysine coated glass bottom dishes and then fixed, stained, and analyzed. Ideally, this sorted population would contain T2 lung cells which are easily visualized. Using confocal microscopy, indeed BMD T2 pneumocytes could be visualized as GFP^+SPC^+ (refer to Figure 11). However, these double positive cells were exceedingly rare and only 5 convincing cells (0.01%) were visualized. In contrast, the positive control GFP+ mouse yielded approximately 25% of cells that were GFP^+SPC^+ while the SPCKO negative control mouse yielded 0% double positive cells. This FACS method represents a 5-fold enrichment (0.01% vs. 0.002%) for our donor-derived T2 cells of interest compared with examining paraffin sections. The successful use of FACS purification to separate, enrich, and visualize BMD lung epithelial cells enabled a significantly more thorough and easier method to analyze the entire lung for rare engraftment events.

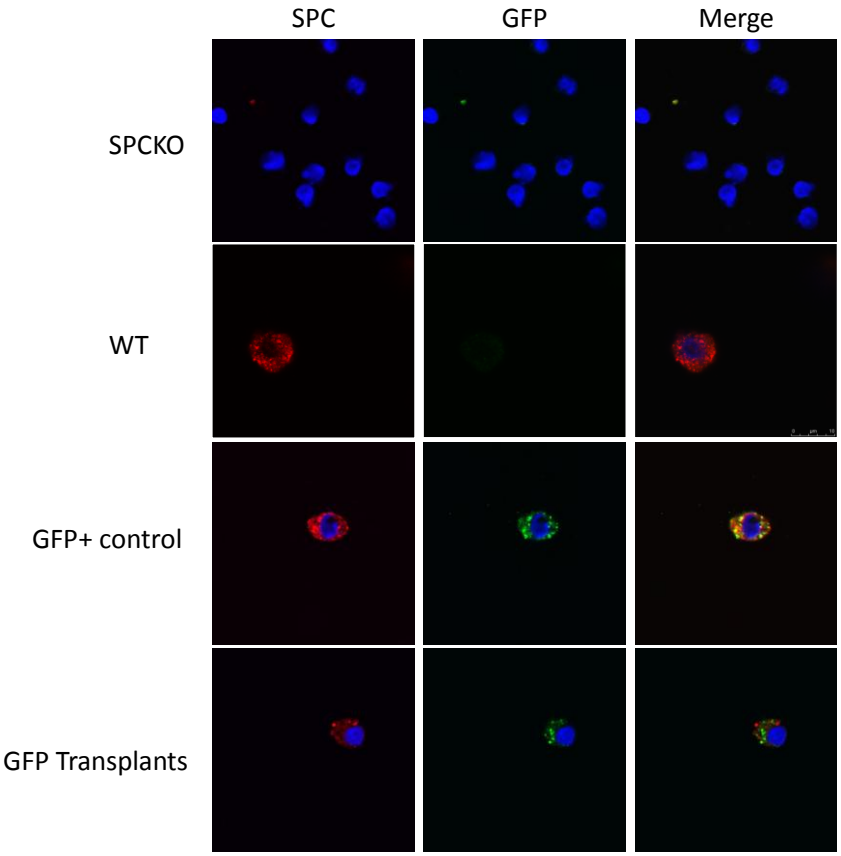

Figure 11: Confocal Microscopy Showing BMD Type II Pneumocytes that Were Purified by FACS

Immunofluorescence of the FACS sorted $CD45^{-}CD11b^{-}CD31^{-}$ population for GFP and SPC. GFP (green) denotes donor derived cells while SPC (red) is the marker for T2 lung cells. Nuclei are stained with DAPI (blue). Double-positive cells ($GFP^{+}SPC^{+}$) could be seen in the GFP transplants, which are suggestive of donor-derived T2 cell engraftment. "SPCKO" is the negative control for SPC and GFP staining. "WT" is the positive control for SPC staining and another negative control for GFP staining. "GFP+ control" is the positive control for both GFP and SPC staining. "GFP Transplants" is the experimental set of GFP-expressing WBM transplanted into a wild type recipient. Images created by Susannah Kassmer using 63X objective magnification.

Engraftment in the Lung May Be Greater Among the Hematopoietic Fraction of BMDCs and May Be Enhanced by a Second Dose of Radiation

As explained in the Introduction and presented in Table 1, there remains an important and ongoing debate concerning which BMD cell population demonstrates the most plasticity. Multiple groups claim that HSCs with their regenerative potential are the cell of interest for these conversions, while others purport that non-hematopoietic MSCs frequently migrate to epithelial tissue and adopt a novel phenotype. In an effort to better describe these cell populations and directly compare their engraftment potential, we made use of vav ancestry mice, which allow the faithful and permanent expression of a YFP transgene if a cell ever expressed the hematopoietic-specific vav promoter. SPCKO recipient mice were lethally irradiated and then systemically administered cells from one of three bone marrow populations isolated from vav-Cre YFP mice: 10^6 unsorted WBM as a positive control, 2 X 10^6 FACS-sorted YFP+ cells representing the hematopoietic fraction, or 5 X 10^5 FACS-sorted YFP- cells representing the non-hematopoietic fraction along with 10^6 SPCKO unsorted WBM (refer to Methods and Figure 2 for details). The third group required supplemental SPCKO WBM because the YFP- population does not otherwise contain hematopoietic cells and without them the irradiated recipient animals would have succumbed to radiation toxicity. The differing number of cells transplanted is the result of the number of cells yielded during FACS sorting. Overall, these differences were not large and should not significantly impact our outcomes. These mice were then sacrificed and evaluated

for lung epithelial engraftment one month later using similar methods to the previous transplants. As before, SPC mRNA and protein were used as reporters for donor-derived cells.

Sex-mismatched transplants were again employed to evaluate hematopoietic engraftment using Y-FISH on bone marrow cytospins. When this blood chimerism was examined by counting 300 cells per slide, all transplanted animals showed greater than 97% engraftment. This extremely robust engraftment means that essentially the entire hematopoietic system was reconstituted by the donor cells. However, the YFP- population cannot truly be evaluated by hematopoietic engraftment since it does not contain blood-forming cells. To solve this problem, we assessed the short-term hematopoietic engraftment of the co-transplanted SPCKO radioprotection cells as a proxy for YFP- cell survival during transplantation. Although this is not an ideal method, it was the only available strategy.

Unfortunately, cytospins of these transplants were unreliable with large amounts of background fluorescence and fragmented cells. Therefore, only paraffin sections of the lung were used for immunofluorescence to detect SPC signal and therefore donor-derived T2 cells. Since most of these mice were transplanted with YFP+ blood cells, we evaluated autofluorescence on these slides before adding primary antibody to ensure that it did not confound the subsequent staining and yield false positive results. Indeed, following antigen retrieval, the native YFP signal produced a very low background which could not be confused with positive staining results in either the blue, green, or red channel.

Surprisingly, the paraffin sections of these transplants yielded no convincing donor-derived T2 pneumocytes in any of the transplantation groups (refer to Table 4). This most likely was the consequence of the small numbers of animals in each group which survived to analysis. Therefore, another investigator in the lab has subsequently replicated these results with the same outcome (data not shown). This was unanticipated since we expected to see the same level of engraftment as during the earlier WT WBM transplantation studies in which 1 out of 4 mice showing signs of donor cell engraftment on paraffin section. However, the vav-Cre YFP WBM group did not have a single $SPC^{+}CD45^{-}F4/80^{-}$ cell by immunofluorescence on paraffin sections. In light of this data, lung cytospins would certainly have been useful to corroborate the negative results.

Faced with these disappointing results, we attempted to enhance any level of conversion by targeting the right lung of the remaining transplantation animals to a second dose of radiation. This salvage strategy was based on the possibility that we had not reached the threshold of injury that is necessary for BMDC engraftment (40). The left lung was shielded from further damage and served as an internal negative control. One month following this second dose of lethal irradiation, the mice were sacrificed and analyzed.

When immunofluorescence on paraffin lung sections of these animals was studied, 1 of 4 animals in the vav-Cre YFP WBM group and 1 of 3 animals in the vav-Cre YFP+ group demonstrated an $SPC^{+}CD45^{-}F4/80^{-}$ cell in the right lung indicative of T2 epithelial engraftment (refer to Table 4). No greater than two engrafted cells

were detected in either animal. None of the internal control left lungs or transplantation control SPCKO→SPCKO lungs showed any donor-derived T2 alveolar cells. Interestingly, both of the YFP WBM and the sorted YFP+ populations contain the hematopoietic elements of the bone marrow and showed signs of engraftment while the non-hematopoietic sorted YFP- population did not. It is also suggestive that the second radiation dose enhanced engraftment but both these conclusions must be tempered by the low animals numbers and lack of statistical significance in this study.

qPCR for SPC Shows a Significant Increase Following Transplantation of the FACS-Sorted YFP+ Population Only In the Mice that Received a Second Dose of Radiation

In an effort to further evaluate and correlate epithelial engraftment levels, qPCR for SPC was used as before. Following RNA isolation and reverse transcription, whole lung cDNA was evaluated by qPCR for the quantity of SPC transcripts in the various transplantation groups. Total genetic content was normalized using the ubiquitous β2-microglobulin gene as the standard. WT served as the positive control and maximal amount of SPC. A group of SPCKO mice which received SPCKO WBM was included as a negative control for irradiation and transplantation itself.

All the mice in the groups that received unsorted vav-Cre YFP WBM or sorted YFP- cells showed minimal levels of SPC signal similar to the negative control

SPCKO→SPCKO transplants (Figure 12). Although the number of control animals is small, the transcript levels of SPC and β2 were consistent with values from subsequent experiments. Both primary and secondary irradiated animals showed similar results and are presented together (Table 4). However, 2 of the 5 mice in the sorted vav-Cre YFP+ group showed significantly higher levels of SPC transcripts ($p=0.009$) in the right lung. Both of these animals had received a secondary dose of targeted right lung irradiation. The mean –Delta C(t) for these two mice were 13.62 and 13.25 compared with 17.20 for the transplantation negative control. This result represents an approximately 13-fold higher level of SPC signal suggesting that the hematopoietic vav-Cre YFP+ population has some engraftment potential as functional T2 pneumocytes in the lung. This greater expression was only present in the right lung of these animals so it is possible that the second dose of radiation enhanced an epithelial engraftment phenotype. Unfortunately, this level of SPC expression still pales in comparison to the WT positive control which is 2×10^7 times greater.

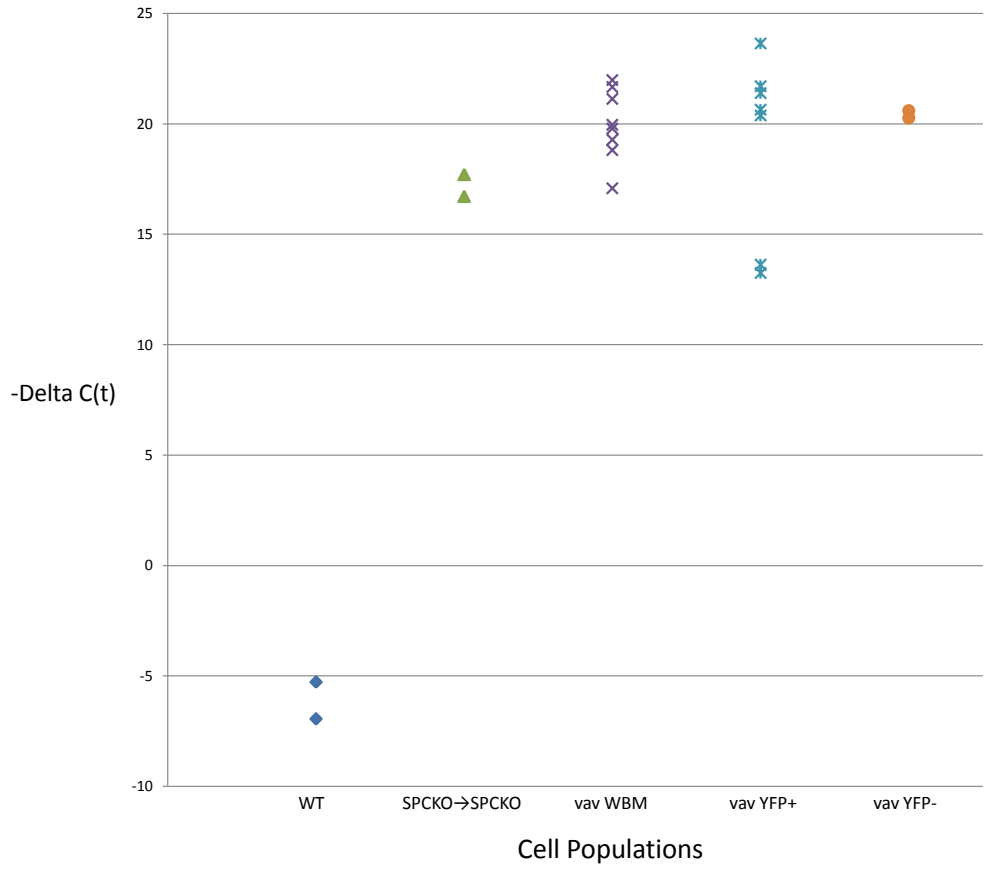

Figure 12: qPCR for SPC Demonstrating Two Animals in the YFP+ Group with Significant Increases in Transcript Levels Suggestive of Engraftment

The vav-Cre YFP WBM and FACS-sorted YFP- transplantation groups showed levels of SPC mRNA consistent with the transplantation negative control SPCKO→SPCKO. But, in the FACS-sorted vav-Cre YFP+ population, 2 mice which both received additional radiation showed significantly greater levels of SPC transcript ($p=0.009$) indicating possible BMD functional T2 cells. Lower –Delta C(t) levels represent more mRNA transcripts. WT is the untransplanted positive control showing normal levels of SPC transcripts. Total RNA content normalized to β2-microglobulin standard. Each dot represents 1 lung with the qPCR performed in triplicate.

Type	Number	X-Ray	Blood Chimerism by Y-FISH	Paraffin	qPCR -Delta C(t)
WBM	978		Positive	Negative	21.66
WBM	980	Y	Positive	Negative	19.27
WBM	985		Positive	Negative	19.79
WBM	986		Positive	Negative	18.80
WBM	987 R	Y	Positive	Positive	19.96
	987 L			Negative	21.98
WBM	995	Y	Positive	Negative	17.08
WBM	990	Y	Positive	Negative	21.12
YFP+	982	Y	Positive	Negative	21.70
YFP+	983 R	Y	Positive	Negative	13.62
	983 L			Negative	20.63
YFP+	991		Positive	Negative	21.38
YFP+	992 R	Y	Positive	Positive	13.25
	992 L			Negative	23.64
YFP+	993		Positive	Negative	20.38
YFP-	984		Positive	Negative	20.60
YFP-	989	Y	Positive	Negative	20.26
SPCKO	SPCKO1		Positive	Negative	17.70
SPCKO	SPCKO2		Positive	Negative	16.71

Table 4: Summary of All Mice Transplanted For the Vav Ancestry and Secondary Irradiation Studies

This table presents an overview of the data from each mouse transplanted in this experimental study. "Type" refers to the population of donor cells transplanted for this group. "Number" is the animal identifier with "R" and "L" meaning right and left lung respectively. "X-ray" represents a second dose of targeted irradiation to the right lung of the mouse. Any animal which showed positive signs of engraftment on either the paraffin sections or qPCR quantification was then compared to the contralateral lung (which represents an internal control). SPCKO is the transplantation negative control of SPCKO WBM while WBM is the transplantation positive control of vav-Cre YFP unsorted WBM. Hematopoietic chimerism, as seen on BM cytospins, was greater than 97% in all animals shown. Paraffin sections of each mouse's lung were quantified as "positive" if donor-derived T2 cells could be identified and "negative" if no cells could be found. The final column shows the raw qPCR data for SPC.

DISCUSSION

Detection Strategies

In an effort to better understand the plasticity and engraftment potential of BMDCs in the lung, we undertook multiple studies to evaluate the presence of donor-derived T2 pneumocytes. The initial weeks of this project were focused on demonstrating our immunofluorescence detection strategy for SPC was viable. Indeed, using a protocol lacking an antigen retrieval step coupled with a guinea pig-raised polyclonal antibody, type II pneumocytes could be consistently recognized by their characteristic vesicular SPC staining during microscopy on both paraffin section and cytospins. These methods were then applied to SPCKO mice which had been lethally irradiated and systemically transplanted with WT WBM. Approximately 24% of these animals demonstrated $SPC^{+}CD45^{-}F4/80^{-}$ T2 cells on microscopy. However, the absolute number of these donor-derived cells was very small with only 0.025% of resident T2 cells being engrafted from the donor. This number was calculated by dividing the mean percentage of SPC+ cells in the transplants by the mean percentage of SPC+ cells in the WT control. Although this minute level of engraftment was reproducibly detectable with our techniques, we realized that additional analyses would be helpful in finding these conversion events.

There were other technical challenges to this phase of the project and thus our interpretation of results. Frequently, we observed different levels of tissue fixation and agarose inflation despite identical methods. Tissue fixation was probably affected by the surface area to volume ratio of each lung as well as time spent in 70% ethanol prior to paraffin embedding. With tissues that were overfixed, the edges of the lung showing high levels of background immunofluorescence. This made the detection of SPC positive cells virtually impossible in certain regions. Although this problem was not extensive, it did obscure a perfectly consistent examination of every slide. During lung preparation, agarose inflation was determined to be an essential step to recapitulate the functionally-relevant inflated architecture of the lung. Unfortunately, this required a tight seal between the angiocatheter and the trachea which was not always possible. The resulting underinflated lungs had high cell densities that distorted morphology and made analysis more difficult due to indistinct cell borders and overlay. By necessity, these questionably positive cells were deemed negative since conclusive microscopic evidence could not be demonstrated. Although these issues made analysis more complicated and skewed toward the negative, they were relatively minor and did not impact our conclusions in any meaningful way.

FLH and LSK Populations

The FLH and LSK transplantation groups showed levels of lung engraftment greater than the control WBM populations when examining immunofluorescence.

This result tentatively suggests that these hematopoietic subpopulations are enriched for cells capable of making the transition to T2 alveolar cells of the lung. However, it is difficult to definitively make these conclusions because of the small numbers of animals and rarity of positive donor-derived cells in these studies. Additional transplantations would be necessary to prove that this outcome is truly significant.

Unfortunately, qPCR data for SPC did not reinforce this trend that FLH and LSK populations showed greater levels of engraftment. But this statistical insignificance was dependent on the negative transplantation control of SPCKO WBM→SPCKO mice. It seems likely that this group was accidentally contaminated during transplantation with WT FLH cells, which were also being isolated and transplanted on the same day. The untransplanted SPCKO mice should have shown the same minimal levels of SPC signal as the negative transplantation control. But our data show a significantly greater level of SPC (greater than 100-fold) in this transplantation group.

An alternative hypothesis for this false upregulation of SPC is that irradiation and transplantation itself (regardless of cell type administered) induces pseudogene expression. Despite the exquisite specificity of the SPC qPCR primer design, it is still possible that an unintended similar target sequence is being amplified erroneously. This hypothesis can be tested using standard gel electrophoresis to confirm that the qPCR product is of the expected 664 base pair size. However, this was not undertaken because of time constraints and the unlikelihood of pseudogene

expression. Since the other transplantation groups (WT WBM and LSK), which were performed on different days, did not show the same effect and clustered around the untransplanted negative control, it is difficult to support this pseudogene theory.

Interestingly, if the SPCKO WBM→SPCKO transplantations were repeated and showed the expected minimum of SPC signal, then the FLH population and a few of the WBM transplants (to a lesser degree) would show significantly higher levels of SPC. This result would correlate with the previous staining data and lend further evidence to the hypothesis that HSC subpopulations are enriched for pluripotent cells capable of epithelial engraftment.

FACS Sorting for Engrafted Type II Pneumocytes

Our investigation showed that FACS sorting the enzymatically digested lung was a viable strategy for selectively isolating lung epithelial cells. In fact, the calculated total number of alveolar cells (24.5%) as well as the number of T2 pneumocytes (6.1%) in the lung compared very favorably with previous estimates using microscopy and immunostaining (20% and 7.9%, respectively). Therefore, this technique allowed us to greatly enrich for alveolar cells such that all possible donor-derived cells of interest could be examined on a single dish. This greatly reduced the likelihood that true engraftment events were missed because of random sampling. Of course, cytospins from these sorts are not the only method that should be applied to these investigations because unfortunately cell morphology and histology are lost during preparation. However, this method does

have the added benefit of reducing overlay artifacts and background immunofluorescence. As we look forward and design future experiments, FACS sorting will certainly be one of the modalities employed to find these extremely rare conversion events.

Vav-Cre Ancestry Populations and Secondary Irradiation

It was surprising that the initial evaluations of engraftment from all three vav ancestry mouse populations were negative by both immunofluorescence and qPCR. However, the fact that a second dose of targeted irradiation was able to induce engraftment subsequently in a few animals suggested that the required threshold of damage was not initially achieved. It is not clear why this second dose was needed in these groups because they initially received sufficient radiation to reconstitute the hematopoietic system with donor cells. However, the use of a contralateral lung control that was shielded from this secondary dose provides strong evidence that the additional radiation was essential for inducing engraftment. In addition to inducing engraftment, these secondarily irradiated animals had subjectively higher levels of tissue damage with an elevated number of macrophages and increased fibrosis. Previous research has shown that the number of SPC-expressing T2 cells typically decreases along with surfactant levels with repeated irradiation (82), which makes it all the more striking that significantly greater levels of engraftment were seen.

Although the numbers of animals used in this study were small, our data hint that the YFP+ hematopoietic components of the bone marrow are able to engraft at

least as well as the control WBM while the YFP- non-hematopoietic cells were not. When taken with the previous conclusions from the LSK and FLH experiments, it looks as if the HSC subpopulation contains the plasticity necessary to engraft as type II pneumocytes in the lung. But before these hypotheses are proven definitively, additional transplantations must be performed especially using the YFP- vav ancestry population. To further enhance these studies and complement the paraffin section and qPCR results, FACS sorting of digested lungs should be employed to provide a reliable and powerful method to find rare donor-derived cells by immunofluorescence.

The Difficulties in Demonstrating Plasticity

Throughout all our transplantation examinations, our detection strategies skew heavily towards the null hypothesis that donor-derived T2 cells do not exist. Transplantation itself places remarkable challenges on the donor cells. They were asked to exist outside of an organism for hours in varying reagents while they were being isolated, purified, and prepared for injection. These transplanted bone marrow cells were then required to home from the vasculature to their natural niche while also competing with the radioprotection SPCKO cells.

Beyond this, engraftment as an epithelial cell required the establishment of an obvious phenotype with wholesale genetic program modifications such that hematopoietic genes were silenced and epithelial markers were upregulated. Specifically, we only detected cells that express the very particular SPC target gene.

In fact, a possible explanation for the low level of SPC signal was its immunologic recognition by the recipient SPC knockout mice as a foreign mRNA and protein. Western blot analysis remains the standard for protein expression studies and would have been utilized here; but previous work demonstrated that SPC protein levels were too low for consistent detection.

Additionally, we utilized a high degree of skepticism when examining every potentially SPC-positive cell. Even the positive control WT mouse had many T2 cells, which would not be considered positive because they weren't definitely clear examples of an SPC-positive staining pattern. This placed a great onus on the engrafted cells to not only express SPC but also express it in the classically recognized morphology. Given all these challenges both biologically and technically, it is amazing that any positive cells could be found.

Additional T2 cell-specific antibodies, such as the nuclearly localized thyroid transcription factor 1 (83) or cytokeratin-7, might be included for future immunofluorescence studies to reduce the ambiguity of certain positive cells. But this carries with it further challenges such as using another non-overlapping color channel for detection. Also it complicates analysis because it reduces the likelihood of finding a cell which definitely and characteristically expresses both phenotype markers.

The Mechanisms of Plasticity

The possible mechanisms responsible for BDMC plasticity remains a hotly debated topic with little consensus in the literature. The first option, which has been already alluded to in the previous section, is transdifferentiation in which one committed cell type has the ability to changes its phenotype and gene expression profile to that of an entirely different cell type. This theory is derived from in vivo studies conducted with plants in which photosynthetic mesophyll cells isolated from zinnia leaves transdifferentiate into xylem cells (84) and with animals in which amphibians such as newts are able to undergo limb regeneration (85). Using in vitro methods, there are also multiple reports of terminally differentiated somatic cell phenotype switching from pancreatic epithelium to hepatocytes (86) and fibroblast to T-cell (87). Most recently, the discovery of and ensuing work with induced pluripotent stem (iPS) cells has deconstructed the idea of non-reversible cell commitment by showing that many mature cell types are able to be transformed into embryonic-like stem cells capable of producing all three germ layers in addition to chimeric animals (88-92).

A priori it is reasonable to hypothesize that systemically delivered BMDC would become entrapped in highly arborized capillary networks such as found in the lung. These donor cells then receive local cellular signals from their newly established niche driving adaptation to the resident tissue. If this mechanism were taking place, it is reasonable to assume that donor derived cells would be found in other capillary networks which is in fact the case as explained in the Introduction. Additionally, a dose response curve would be evident such that greater levels of

epithelial engraftment would be seen with greater numbers of cells transplanted. This experiment has yet to be performed but it offers an opportunity to examine this hypothesis. Our work does not show a clear correlation between donor hematopoietic reconstitution and levels of epithelial engraftment but these outcome measures may be unrelated to transdifferentiation capacity.

Alternatively, there could be a previously undescribed highly pluripotent BMDC population that has not committed to becoming blood and therefore has the ability to self-renew as well as differentiate into hematopoietic stem cells and epithelial cell lineages. Among the suspected populations are multipotent adult progenitor cells (MAPCs)(93) and very small embryonic-like cells (VSELs)(94, 95).

The third possible mechanism for plasticity could be the fusion of a BMDC with a non-hematopoietic cell to form a heterokaryon, which has the gene expression profile of the fusion partner. The two most documented examples are: when a fibroblast fuses with a myoblast to form a heterokaryon, the fibroblast nuclei expresses muscle-specific mRNA (96), and during somatic cell nuclear transfer into unfertilized oocytes, the somatic nuclei undergoes nearly complete reprogramming (97). More recent data have shown that macrophages have the ability to fuse with injured hepatocytes in vivo and that the resulting macrophage nucleus expresses liver-specific transcripts (98, 99). Lastly, previous work in the lab has shown that 20-50% of BMD epithelial cells in the lung are due to fusion (100). Therefore, fusion has been shown to be a mechanism by which this conversion takes places but this does not preclude that other possible mechanisms aren't involved.

The fourth possibility is based on the newly discovered capacity of cells to take up microvesicles containing mRNA from other cells (101). This transferred mRNA can then be detected along with its translated protein in the recipient cell (102). In fact, uptake and expression of lung epithelial cell-derived mRNA by co-cultured BMDCs has been demonstrated (103).

Future Directions

Of course, this thesis represents a work in progress and additional experiments await completion in order to more fully develop an understanding of the plasticity of bone marrow derived cells. Questions regarding the kinetics of this transformation process are still unanswered. "How long does this transition take?" and "How does the number of engrafted cells change over time?" are relevant questions which need to be investigated. As discussed in the Introduction, the transplantation of BMDCs appears to have the greatest clinical benefit in an acute setting. It seems unlikely that the very low numbers of BMD engrafted cells could provide a lasting functional benefit. However, how these cells interact with the native tissue in a long time course has yet to be studied. In order to examine these questions, we would like to conduct a longitudinal study to examine engraftment at multiple time points. Using the same methods to complement our three month post-transplantation time point, engraftment data should be collected one week, one month, six months, and one year after transplantation. The FACS sorting of potential cells could be of the most benefit here since it was reliable and sensitive enough to

provide a quantitative measure of these events. I predict that the greatest number of engrafted cells would be detected in the first week post-irradiation when there is large scale apoptosis and high levels of circulating cytokines and growth factors. I suspect that after this initial event the number of engrafted cells drops precipitously such that at one year no donor-derived epithelial cells can be detected.

The LSK, FLH, and vav-Cre YFP+ hematopoietic populations engrafted at least as well as WBM in the lungs of transplanted animals. However, these well studied subpopulations represent a small fraction of the purported stem cell populations present in the bone marrow. Future experiments would focus on rigorously studying other bone marrow subpopulations, perhaps not of the hematopoietic lineage, in order to assess their epithelial plasticity in the lung. In particular, plasticity experiments involving mesenchymal stem cells (MSC), very small embryonic-like cells (VSEL), side population cells, and amniotic fluid stem cells are among the many being discussed in the literature. These populations may hold exceptional transformation properties as multiple groups have already demonstrated their multipotent capability (104-108). Essentially, the future directions of this project will focus on pursuing a starting population of cells which have the most potential for therapeutic relevance using tissue engineering principles. Specifically, we will search for the cells type that has the most robust ability to home sites of injury and contribute to in vivo tissue repair.

REFERENCES

1. Kumar, V., Abbas, A.K., Fausto, N., Robbins, S.L., and Cotran, R.S. 2005. *Robbins and Cotran pathologic basis of disease*. Philadelphia: Elsevier Saunders. xv, 1525 p. pp.
2. Boron, W.F., and Boulpaep, E.L. 2005. *Medical physiology : a cellular and molecular approach*. Philadelphia, Pa.: Elsevier Saunders. xiii, 1319 p. pp.
3. Hermans, C., and Bernard, A. 1999. Lung epithelium-specific proteins: characteristics and potential applications as markers. *Am J Respir Crit Care Med* 159:646-678.
4. Clark, J.C., Wert, S.E., Bachurski, C.J., Stahlman, M.T., Stripp, B.R., Weaver, T.E., and Whitsett, J.A. 1995. Targeted disruption of the surfactant protein B gene disrupts surfactant homeostasis, causing respiratory failure in newborn mice. *Proc Natl Acad Sci U S A* 92:7794-7798.
5. Nogee, L.M., Garnier, G., Dietz, H.C., Singer, L., Murphy, A.M., deMello, D.E., and Colten, H.R. 1994. A mutation in the surfactant protein B gene responsible for fatal neonatal respiratory disease in multiple kindreds. *J Clin Invest* 93:1860-1863.
6. Glasser, S.W., Burhans, M.S., Korfhagen, T.R., Na, C.L., Sly, P.D., Ross, G.F., Ikegami, M., and Whitsett, J.A. 2001. Altered stability of pulmonary surfactant in SP-C-deficient mice. *Proc Natl Acad Sci U S A* 98:6366-6371.
7. Glasser, S.W., Detmer, E.A., Ikegami, M., Na, C.L., Stahlman, M.T., and Whitsett, J.A. 2003. Pneumonitis and emphysema in sp-C gene targeted mice. *J Biol Chem* 278:14291-14298.
8. Weissman, I.L. 2000. Translating stem and progenitor cell biology to the clinic: barriers and opportunities. *Science* 287:1442-1446.
9. Muller-Sieburg, C.E., Whitlock, C.A., and Weissman, I.L. 1986. Isolation of two early B lymphocyte progenitors from mouse marrow: a committed pre-pre-B cell and a clonogenic Thy-1-lo hematopoietic stem cell. *Cell* 44:653-662.
10. Till, J.E., and McCulloch, E. 1961. A direct measurement of the radiation sensitivity of normal mouse bone marrow cells. *Radiat Res* 14:213-222.
11. Jordan, C.T., and Lemischka, I.R. 1990. Clonal and systemic analysis of long-term hematopoiesis in the mouse. *Genes Dev* 4:220-232.
12. Lemieux, M.E., Rebel, V.I., Lansdorp, P.M., and Eaves, C.J. 1995. Characterization and purification of a primitive hematopoietic cell type in adult mouse marrow capable of lymphomyeloid differentiation in long-term marrow "switch" cultures. *Blood* 86:1339-1347.
13. Pawliuk, R., Eaves, C., and Humphries, R.K. 1996. Evidence of both ontogeny and transplant dose-regulated expansion of hematopoietic stem cells in vivo. *Blood* 88:2852-2858.
14. Szilvassy, S.J., Humphries, R.K., Lansdorp, P.M., Eaves, A.C., and Eaves, C.J. 1990. Quantitative assay for totipotent reconstituting hematopoietic stem

cells by a competitive repopulation strategy. *Proc Natl Acad Sci U S A* 87:8736-8740.
15. Krause, D.S., Ito, T., Fackler, M.J., Smith, O.M., Collector, M.I., Sharkis, S.J., and May, W.S. 1994. Characterization of murine CD34, a marker for hematopoietic progenitor and stem cells. *Blood* 84:691-701.
16. Morrison, S.J., Wandycz, A.M., Hemmati, H.D., Wright, D.E., and Weissman, I.L. 1997. Identification of a lineage of multipotent hematopoietic progenitors. *Development* 124:1929-1939.
17. Wolf, N.S., Kone, A., Priestley, G.V., and Bartelmez, S.H. 1993. In vivo and in vitro characterization of long-term repopulating primitive hematopoietic cells isolated by sequential Hoechst 33342-rhodamine 123 FACS selection. *Exp Hematol* 21:614-622.
18. Lanzkron, S.M., Collector, M.I., and Sharkis, S.J. 1999. Hematopoietic stem cell tracking in vivo: a comparison of short-term and long-term repopulating cells. *Blood* 93:1916-1921.
19. Krause, D.S., Theise, N.D., Collector, M.I., Henegariu, O., Hwang, S., Gardner, R., Neutzel, S., and Sharkis, S.J. 2001. Multi-organ, multi-lineage engraftment by a single bone marrow-derived stem cell. *Cell* 105:369-377.
20. Kotton, D.N., Ma, B.Y., Cardoso, W.V., Sanderson, E.A., Summer, R.S., Williams, M.C., and Fine, A. 2001. Bone marrow-derived cells as progenitors of lung alveolar epithelium. *Development* 128:5181-5188.
21. Grove, J.E., Lutzko, C., Priller, J., Henegariu, O., Theise, N.D., Kohn, D.B., and Krause, D.S. 2002. Marrow-derived cells as vehicles for delivery of gene therapy to pulmonary epithelium. *Am J Respir Cell Mol Biol* 27:645-651.
22. Theise, N.D., Henegariu, O., Grove, J., Jagirdar, J., Kao, P.N., Crawford, J.M., Badve, S., Saxena, R., and Krause, D.S. 2002. Radiation pneumonitis in mice: a severe injury model for pneumocyte engraftment from bone marrow. *Exp Hematol* 30:1333-1338.
23. Ortiz, L.A., Gambelli, F., McBride, C., Gaupp, D., Baddoo, M., Kaminski, N., and Phinney, D.G. 2003. Mesenchymal stem cell engraftment in lung is enhanced in response to bleomycin exposure and ameliorates its fibrotic effects. *Proc Natl Acad Sci U S A* 100:8407-8411.
24. Orlic, D., Kajstura, J., Chimenti, S., Jakoniuk, I., Anderson, S.M., Li, B., Pickel, J., McKay, R., Nadal-Ginard, B., Bodine, D.M., et al. 2001. Bone marrow cells regenerate infarcted myocardium. *Nature* 410:701-705.
25. Eglitis, M.A., and Mezey, E. 1997. Hematopoietic cells differentiate into both microglia and macroglia in the brains of adult mice. *Proc Natl Acad Sci U S A* 94:4080-4085.
26. Ferrari, G., Cusella-De Angelis, G., Coletta, M., Paolucci, E., Stornaiuolo, A., Cossu, G., and Mavilio, F. 1998. Muscle regeneration by bone marrow-derived myogenic progenitors. *Science* 279:1528-1530.
27. Gussoni, E., Soneoka, Y., Strickland, C.D., Buzney, E.A., Khan, M.K., Flint, A.F., Kunkel, L.M., and Mulligan, R.C. 1999. Dystrophin expression in the mdx mouse restored by stem cell transplantation. *Nature* 401:390-394.
28. Hou, Z., Nguyen, Q., Frenkel, B., Nilsson, S.K., Milne, M., van Wijnen, A.J., Stein, J.L., Quesenberry, P., Lian, J.B., and Stein, G.S. 1999. Osteoblast-specific gene

expression after transplantation of marrow cells: implications for skeletal gene therapy. *Proc Natl Acad Sci U S A* 96:7294-7299.
29. Alison, M.R., Poulsom, R., Jeffery, R., Dhillon, A.P., Quaglia, A., Jacob, J., Novelli, M., Prentice, G., Williamson, J., and Wright, N.A. 2000. Hepatocytes from non-hepatic adult stem cells. *Nature* 406:257.
30. Petersen, B.E., Bowen, W.C., Patrene, K.D., Mars, W.M., Sullivan, A.K., Murase, N., Boggs, S.S., Greenberger, J.S., and Goff, J.P. 1999. Bone marrow as a potential source of hepatic oval cells. *Science* 284:1168-1170.
31. Gupta, S., Verfaillie, C., Chmielewski, D., Kim, Y., and Rosenberg, M.E. 2002. A role for extrarenal cells in the regeneration following acute renal failure. *Kidney Int* 62:1285-1290.
32. Poulsom, R., Forbes, S.J., Hodivala-Dilke, K., Ryan, E., Wyles, S., Navaratnarasah, S., Jeffery, R., Hunt, T., Alison, M., Cook, T., et al. 2001. Bone marrow contributes to renal parenchymal turnover and regeneration. *J Pathol* 195:229-235.
33. Ianus, A., Holz, G.G., Theise, N.D., and Hussain, M.A. 2003. In vivo derivation of glucose-competent pancreatic endocrine cells from bone marrow without evidence of cell fusion. *J Clin Invest* 111:843-850.
34. Hess, D., Li, L., Martin, M., Sakano, S., Hill, D., Strutt, B., Thyssen, S., Gray, D.A., and Bhatia, M. 2003. Bone marrow-derived stem cells initiate pancreatic regeneration. *Nat Biotechnol* 21:763-770.
35. Harris, J.R., Brown, G.A., Jorgensen, M., Kaushal, S., Ellis, E.A., Grant, M.B., and Scott, E.W. 2006. Bone marrow-derived cells home to and regenerate retinal pigment epithelium after injury. *Invest Ophthalmol Vis Sci* 47:2108-2113.
36. Badiavas, E.V., Abedi, M., Butmarc, J., Falanga, V., and Quesenberry, P. 2003. Participation of bone marrow derived cells in cutaneous wound healing. *J Cell Physiol* 196:245-250.
37. Herzog, E.L., Chai, L., and Krause, D.S. 2003. Plasticity of marrow-derived stem cells. *Blood* 102:3483-3493.
38. Theise, N.D., Badve, S., Saxena, R., Henegariu, O., Sell, S., Crawford, J.M., and Krause, D.S. 2000. Derivation of hepatocytes from bone marrow cells in mice after radiation-induced myeloablation. *Hepatology* 31:235-240.
39. Herzog, E.L., and Krause, D.S. 2006. Engraftment of marrow-derived epithelial cells: the role of fusion. *Proc Am Thorac Soc* 3:691-695.
40. Herzog, E.L., Van Arnam, J., Hu, B., and Krause, D.S. 2006. Threshold of lung injury required for the appearance of marrow-derived lung epithelia. *Stem Cells* 24:1986-1992.
41. Jones, A.W., and Reeve, N.L. 1978. Ultrastructural study of bleomycin-induced pulmonary changes in mice. *J Pathol* 124:227-233.
42. Pereira, R.F., Halford, K.W., O'Hara, M.D., Leeper, D.B., Sokolov, B.P., Pollard, M.D., Bagasra, O., and Prockop, D.J. 1995. Cultured adherent cells from marrow can serve as long-lasting precursor cells for bone, cartilage, and lung in irradiated mice. *Proc Natl Acad Sci U S A* 92:4857-4861.
43. Wagers, A.J., Sherwood, R.I., Christensen, J.L., and Weissman, I.L. 2002. Little evidence for developmental plasticity of adult hematopoietic stem cells. *Science* 297:2256-2259.

44. van Haaften, T., and Thebaud, B. 2006. Adult bone marrow-derived stem cells for the lung: implications for pediatric lung diseases. *Pediatr Res* 59:94R-99R.
45. Kotton, D.N., Fabian, A.J., and Mulligan, R.C. 2005. Failure of bone marrow to reconstitute lung epithelium. *Am J Respir Cell Mol Biol* 33:328-334.
46. Chang, J.C., Summer, R., Sun, X., Fitzsimmons, K., and Fine, A. 2005. Evidence that bone marrow cells do not contribute to the alveolar epithelium. *Am J Respir Cell Mol Biol* 33:335-342.
47. Swenson, E.S., Price, J.G., Brazelton, T., and Krause, D.S. 2007. Limitations of green fluorescent protein as a cell lineage marker. *Stem Cells* 25:2593-2600.
48. Spees, J.L., Olson, S.D., Ylostalo, J., Lynch, P.J., Smith, J., Perry, A., Peister, A., Wang, M.Y., and Prockop, D.J. 2003. Differentiation, cell fusion, and nuclear fusion during ex vivo repair of epithelium by human adult stem cells from bone marrow stroma. *Proc Natl Acad Sci U S A* 100:2397-2402.
49. Rojas, M., Xu, J., Woods, C.R., Mora, A.L., Spears, W., Roman, J., and Brigham, K.L. 2005. Bone marrow-derived mesenchymal stem cells in repair of the injured lung. *Am J Respir Cell Mol Biol* 33:145-152.
50. Wang, G., Bunnell, B.A., Painter, R.G., Quiniones, B.C., Tom, S., Lanson, N.A., Jr., Spees, J.L., Bertucci, D., Peister, A., Weiss, D.J., et al. 2005. Adult stem cells from bone marrow stroma differentiate into airway epithelial cells: Potential therapy for cystic fibrosis. *Proc Natl Acad Sci U S A* 102:186-191.
51. Loi, R., Beckett, T., Goncz, K.K., Suratt, B.T., and Weiss, D.J. 2005. Limited Restoration of Cystic Fibrosis Lung Epithelium in vivo with Adult Marrow Derived Cells. *Am J Respir Crit Care Med* 173:171-179.
52. Xu, J., Woods, C.R., Mora, A.L., Joodi, R., Brigham, K.L., Iyer, S., and Rojas, M. 2007. Prevention of endotoxin-induced systemic response by bone marrow-derived mesenchymal stem cells in mice. *Am J Physiol Lung Cell Mol Physiol* 293:L131-141.
53. Wong, A.P., Dutly, A.E., Sacher, A., Lee, H., Hwang, D.M., Liu, M., Keshavjee, S., Hu, J., and Waddell, T.K. 2007. Targeted cell replacement with bone marrow cells for airway epithelial regeneration. *Am J Physiol Lung Cell Mol Physiol* 293:L740-752.
54. Theise, N., Henegariu, O., Grove, J., Jagirdar, J., Kao, P., Crawford, J., Badve, S., Saxena, R., and Krause, D. 2002. Radiation pneumonitis in mice: A severe injury model for pneumocyte engraftment from bone marrow. *Exp Hematol* 30:1333-1338.
55. Yamada, M., Kubo, H., Kobayashi, S., Ishizawa, K., Numasaki, M., Ueda, S., Suzuki, T., and Sasaki, H. 2004. Bone marrow-derived progenitor cells are important for lung repair after lipopolysaccharide-induced lung injury. *J Immunol* 172:1266-1272.
56. Macpherson, H., Keir, P., Webb, S., Samuel, K., Boyle, S., Bickmore, W., Forrester, L., and Dorin, J. 2005. Bone marrow-derived SP cells can contribute to the respiratory tract of mice in vivo. *J Cell Sci* 118:2441-2450.
57. Spees, J.L., Pociask, D.A., Sullivan, D.E., Whitney, M.J., Lasky, J.A., Prockop, D.J., and Brody, A.R. 2007. Engraftment of Bone Marrow Progenitor Cells in a Rat Model of Asbestos-Induced Pulmonary Fibrosis. *Am J Respir Crit Care Med*.

58. Suratt, B.T., Cool, C.D., Serls, A.E., Chen, L., Varella-Garcia, M., Shpall, E.J., Brown, K.K., and Worthen, G.S. 2003. Human pulmonary chimerism after hematopoietic stem cell transplantation. *Am J Respir Crit Care Med* 168:318-322.
59. Abe, S., Lauby, G., Boyer, C., Rennard, S.I., and Sharp, J.G. 2003. Transplanted BM and BM side population cells contribute progeny to the lung and liver in irradiated mice. *Cytotherapy* 5:523-533.
60. Ishizawa, K., Kubo, H., Yamada, M., Kobayashi, S., Numasaki, M., Ueda, S., Suzuki, T., and Sasaki, H. 2004. Bone marrow-derived cells contribute to lung regeneration after elastase-induced pulmonary emphysema. *FEBS Lett* 556:249-252.
61. Abe, S., Boyer, C., Liu, X., Wen, F.Q., Kobayashi, T., Fang, Q., Wang, X., Hashimoto, M., Sharp, J.G., and Rennard, S.I. 2004. Cells derived from the circulation contribute to the repair of lung injury. *Am J Respir Crit Care Med* 170:1158-1163.
62. Gomperts, B.N., Belperio, J.A., Rao, P.N., Randell, S.H., Fishbein, M.C., Burdick, M.D., and Strieter, R.M. 2006. Circulating progenitor epithelial cells traffic via CXCR4/CXCL12 in response to airway injury. *J Immunol* 176:1916-1927.
63. Serrano-Mollar, A., Nacher, M., Gay-Jordi, G., Closa, D., Xaubet, A., and Bulbena, O. 2007. Intratracheal transplantation of alveolar type II cells reverses bleomycin-induced lung fibrosis. *Am J Respir Crit Care Med* 176:1261-1268.
64. Spencer, H., Rampling, D., Aurora, P., Bonnet, D., Hart, S.L., and Jaffe, A. 2005. Transbronchial biopsies provide longitudinal evidence for epithelial chimerism in children following sex mismatched lung transplantation. *Thorax* 60:60-62.
65. Kleeberger, W., Versmold, A., Rothamel, T., Glockner, S., Bredt, M., Haverich, A., Lehmann, U., and Kreipe, H. 2003. Increased chimerism of bronchial and alveolar epithelium in human lung allografts undergoing chronic injury. *Am J Pathol* 162:1487-1494.
66. Krause, D.S. 2008. Bone marrow-derived cells and stem cells in lung repair. *Proc Am Thorac Soc* 5:323-327.
67. Theise, N.D., Nimmakayalu, M., Gardner, R., Illei, P.B., Morgan, G., Teperman, L., Henegariu, O., and Krause, D.S. 2000. Liver from bone marrow in humans. *Hepatology* 32:11-16.
68. Zander, D.S., Baz, M.A., Cogle, C.R., Visner, G.A., Theise, N.D., and Crawford, J.M. 2005. Bone marrow-derived stem-cell repopulation contributes minimally to the Type II pneumocyte pool in transplanted human lungs. *Transplantation* 80:206-212.
69. Lemischka, I. 2002. A few thoughts about the plasticity of stem cells. *Exp Hematol* 30:848-852.
70. Lagasse, E., Connors, H., Al-Dhalimy, M., Reitsma, M., Dohse, M., Osborne, L., Wang, X., Finegold, M., Weissman, I.L., and Grompe, M. 2000. Purified hematopoietic stem cells can differentiate into hepatocytes in vivo. *Nat Med* 6:1229-1234.

71. Orlic, D., Kajstura, J., Chimenti, S., Bodine, D.M., Leri, A., and Anversa, P. 2001. Transplanted adult bone marrow cells repair myocardial infarcts in mice. *Ann N Y Acad Sci* 938:221-229; discussion 229-230.
72. Orlic, D., Kajstura, J., Chimenti, S., Limana, F., Jakoniuk, I., Quaini, F., Nadal-Ginard, B., Bodine, D.M., Leri, A., and Anversa, P. 2001. Mobilized bone marrow cells repair the infarcted heart, improving function and survival. *Proc Natl Acad Sci U S A* 98:10344-10349.
73. Bruscia, E.M., Price, J.E., Cheng, E.C., Weiner, S., Caputo, C., Ferreira, E.C., Egan, M.E., and Krause, D.S. 2006. Assessment of cystic fibrosis transmembrane conductance regulator (CFTR) activity in CFTR-null mice after bone marrow transplantation. *Proc Natl Acad Sci U S A* 103:2965-2970.
74. Zhao, L.R., Duan, W.M., Reyes, M., Keene, C.D., Verfaillie, C.M., and Low, W.C. 2002. Human bone marrow stem cells exhibit neural phenotypes and ameliorate neurological deficits after grafting into the ischemic brain of rats. *Exp Neurol* 174:11-20.
75. Kale, S., Karihaloo, A., Clark, P.R., Kashgarian, M., Krause, D.S., and Cantley, L.G. 2003. Bone marrow stem cells contribute to repair of the ischemically injured renal tubule. *J Clin Invest* 112:42-49.
76. Bustelo, X.R. 2001. Vav proteins, adaptors and cell signaling. *Oncogene* 20:6372-6381.
77. Stadtfeld, M., and Graf, T. 2005. Assessing the role of hematopoietic plasticity for endothelial and hepatocyte development by non-invasive lineage tracing. *Development* 132:203-213.
78. Morrison, S.J., and Weissman, I.L. 1994. The long-term repopulating subset of hematopoietic stem cells is deterministic and isolatable by phenotype. *Immunity* 1:661-673.
79. Corti, M., Brody, A.R., and Harrison, J.H. 1996. Isolation and primary culture of murine alveolar type II cells. *Am J Respir Cell Mol Biol* 14:309-315.
80. Richards, R.J., Davies, N., Atkins, J., and Oreffo, V.I. 1987. Isolation, biochemical characterization, and culture of lung type II cells of the rat. *Lung* 165:143-158.
81. Juopperi, T.A., Schuler, W., Yuan, X., Collector, M.I., Dang, C.V., and Sharkis, S.J. 2007. Isolation of Bone Marrow-Derived Stem Cells using Density-Gradient Separation. *Experimental Hematology* 35:335-341.
82. Rubin, P., Siemann, D.W., Shapiro, D.L., Finkelstein, J.N., and Penney, D.P. 1983. Surfactant release as an early measure of radiation pneumonitis. *Int J Radiat Oncol Biol Phys* 9:1669-1673.
83. Holzinger, A., Dingle, S., Bejarano, P.A., Miller, M.A., Weaver, T.E., DiLauro, R., and Whitsett, J.A. 1996. Monoclonal antibody to thyroid transcription factor-1: production, characterization, and usefulness in tumor diagnosis. *Hybridoma* 15:49-53.
84. Demura, T., Tashiro, G., Horiguchi, G., Kishimoto, N., Kubo, M., Matsuoka, N., Minami, A., Nagata-Hiwatashi, M., Nakamura, K., Okamura, Y., et al. 2002. Visualization by comprehensive microarray analysis of gene expression programs during transdifferentiation of mesophyll cells into xylem cells. *Proc Natl Acad Sci U S A* 99:15794-15799.

85. Stocum, D.L. 2002. Development. A tail of transdifferentiation. *Science* 298:1901-1903.
86. Shen, C.N., Slack, J.M., and Tosh, D. 2000. Molecular basis of transdifferentiation of pancreas to liver. *Nat Cell Biol* 2:879-887.
87. Hakelien, A.M., Landsverk, H.B., Robl, J.M., Skalhegg, B.S., and Collas, P. 2002. Reprogramming fibroblasts to express T-cell functions using cell extracts. *Nat Biotechnol* 20:460-466.
88. Takahashi, K., and Yamanaka, S. 2006. Induction of pluripotent stem cells from mouse embryonic and adult fibroblast cultures by defined factors. *Cell* 126:663-676.
89. Hanna, J., Markoulaki, S., Schorderet, P., Carey, B.W., Beard, C., Wernig, M., Creyghton, M.P., Steine, E.J., Cassady, J.P., Foreman, R., et al. 2008. Direct reprogramming of terminally differentiated mature B lymphocytes to pluripotency. *Cell* 133:250-264.
90. Aoi, T., Yae, K., Nakagawa, M., Ichisaka, T., Okita, K., Takahashi, K., Chiba, T., and Yamanaka, S. 2008. Generation of pluripotent stem cells from adult mouse liver and stomach cells. *Science* 321:699-702.
91. Wernig, M., Lengner, C.J., Hanna, J., Lodato, M.A., Steine, E., Foreman, R., Staerk, J., Markoulaki, S., and Jaenisch, R. 2008. A drug-inducible transgenic system for direct reprogramming of multiple somatic cell types. *Nat Biotechnol* 26:916-924.
92. Eminli, S., Utikal, J., Arnold, K., Jaenisch, R., and Hochedlinger, K. 2008. Reprogramming of neural progenitor cells into induced pluripotent stem cells in the absence of exogenous Sox2 expression. *Stem Cells* 26:2467-2474.
93. Jiang, Y., Jahagirdar, B.N., Reinhardt, R.L., Schwartz, R.E., Keene, C.D., Ortiz-Gonzalez, X.R., Reyes, M., Lenvik, T., Lund, T., Blackstad, M., et al. 2002. Pluripotency of mesenchymal stem cells derived from adult marrow. *Nature* 418:41-49.
94. Ratajczak, J., Miekus, K., Kucia, M., Zhang, J., Reca, R., Dvorak, P., and Ratajczak, M.Z. 2006. Embryonic stem cell-derived microvesicles reprogram hematopoietic progenitors: evidence for horizontal transfer of mRNA and protein delivery. *Leukemia* 20:847-856.
95. Kucia, M., Reca, R., Campbell, F.R., Zuba-Surma, E., Majka, M., Ratajczak, J., and Ratajczak, M.Z. 2006. A population of very small embryonic-like (VSEL) CXCR4(+)SSEA-1(+)Oct-4+ stem cells identified in adult bone marrow. *Leukemia* 20:857-869.
96. Hardeman, E.C., Chiu, C.P., Minty, A., and Blau, H.M. 1986. The pattern of actin expression in human fibroblast x mouse muscle heterokaryons suggests that human muscle regulatory factors are produced. *Cell* 47:123-130.
97. Willadsen, S.M. 1986. Nuclear transplantation in sheep embryos. *Nature* 320:63-65.
98. Vassilopoulos, G., Wang, P.R., and Russell, D.W. 2003. Transplanted bone marrow regenerates liver by cell fusion. *Nature* 422:901-904.
99. Wang, X., Willenbring, H., Akkari, Y., Torimaru, Y., Foster, M., Al-Dhalimy, M., Lagasse, E., Finegold, M., Olson, S., and Grompe, M. 2003. Cell fusion is the principal source of bone-marrow-derived hepatocytes. *Nature* 422:897-901.

100. Herzog, E.L., Van Arnam, J., Hu, B., Zhang, J., Chen, Q., Haberman, A.M., and Krause, D.S. 2007. Lung-specific nuclear reprogramming is accompanied by heterokaryon formation and Y chromosome loss following bone marrow transplantation and secondary inflammation. *FASEB J* 21:2592-2601.
101. Baj-Krzyworzeka, M., Szatanek, R., Weglarczyk, K., Baran, J., Urbanowicz, B., Branski, P., Ratajczak, M.Z., and Zembala, M. 2006. Tumour-derived microvesicles carry several surface determinants and mRNA of tumour cells and transfer some of these determinants to monocytes. *Cancer Immunol Immunother* 55:808-818.
102. Ratajczak, J., Wysoczynski, M., Hayek, F., Janowska-Wieczorek, A., and Ratajczak, M.Z. 2006. Membrane-derived microvesicles: important and underappreciated mediators of cell-to-cell communication. *Leukemia* 20:1487-1495.
103. Aliotta, J.M., Sanchez-Guijo, F.M., Dooner, G.J., Johnson, K.W., Dooner, M.S., Greer, K.A., Greer, D., Pimentel, J., Kolankiewicz, L.M., Puente, N., et al. 2007. Alteration of marrow cell gene expression, protein production, and engraftment into lung by lung-derived microvesicles: a novel mechanism for phenotype modulation. *Stem Cells* 25:2245-2256.
104. Cananzi, M., Atala, A., and De Coppi, P. 2009. Stem cells derived from amniotic fluid: new potentials in regenerative medicine. *Reprod Biomed Online* 18 Suppl 1:17-27.
105. Ratajczak, M.Z., Zuba-Surma, E.K., Shin, D.-M., Ratajczak, J., and Kucia, M. 2008. Very small embryonic-like (VSEL) stem cells in adult organs and their potential role in rejuvenation of tissues and longevity. *Experimental Gerontology* 43:1009-1017.
106. Prockop, D.J. 1997. Marrow Stromal Cells as Stem Cells for Nonhematopoietic Tissues. *Science* 276:71-74.
107. Carraro, G., Perin, L., Sedrakyan, S., Giuliani, S., Tiozzo, C., Lee, J., Turcatel, G., Langhe, S.P.D., Driscoll, B., Bellusci, S., et al. 2008. Human Amniotic Fluid Stem Cells Can Integrate and Differentiate into Epithelial Lung Lineages. *Stem Cells* 26:2902-2911.
108. Ohishi, M., and Schipani, E. 2010. Bone marrow mesenchymal stem cells. *J Cell Biochem* 109:277-282.